

# CH(phenol)-bridged bis(imino)pyridines as compartmental supports for diiron precatalysts for ethylene polymerization: exploring cooperative effects on performance

Qiang Chen,<sup>†</sup> Wenjuan Zhang,<sup>†,‡,\*</sup> Gregory A. Solan,<sup>†,§,\*</sup> Randi Zhang,<sup>†</sup> Liwei Guo,<sup>‡</sup> Xiang Hao,<sup>†</sup> and Wen-Hua Sun<sup>†,#,\*</sup>

<sup>†</sup> Key Laboratory of Engineering Plastics, Institute of Chemistry, Chinese Academy of Sciences, Beijing 100190, China. E-mail: whsun@iccas.ac.cn.

<sup>‡</sup> School of Materials Science and Engineering, Beijing Institute of Fashion Technology, Beijing 100029, China. E-mail: zhangwj@bift.edu.cn

<sup>§</sup> Department of Chemistry, University of Leicester, University Road, Leicester LE1 7RH, UK. E-mail: gas8@le.ac.uk

<sup>#</sup> State Key Laboratory for Oxo Synthesis and Selective Oxidation, Lanzhou Institute of Chemical Physics, Chinese Academy of Sciences, Lanzhou 730000, China

**ABSTRACT:** A family of six CH(phenol)-bridged bimetallic bis(imino)pyridine-iron(II) chlorides,  $\text{CH}(\text{C}_6\text{H}_4\text{-4-OH})\{2'-(4\text{-C}_6\text{H}_2\text{-2,6-(R}^1\text{)}_2\text{N}=\text{CMe})\text{-6'-(2'',6''-(R}^2\text{)}_2\text{-4-(R}^3\text{)C}_6\text{H}_2\text{N}=\text{CMe})\text{C}_5\text{H}_3\text{N}\}_2\text{Fe}_2\text{Cl}_4$  [ $\text{R}^1 = \text{R}^2 = \text{Me}$ ,  $\text{R}^3 = \text{H}$  **Fe1**;  $\text{R}^1 = \text{R}^2 = \text{Et}$ ,  $\text{R}^3 = \text{H}$  **Fe2**;  $\text{R}^1 = \text{Me}$ ,  $\text{R}^2 = \text{Et}$ ,  $\text{R}^3 = \text{H}$  **Fe3**;  $\text{R}^1 = \text{Me}$ ,  $\text{R}^2 = i\text{-Pr}$ ,  $\text{R}^3 = \text{H}$  **Fe4**;  $\text{R}^1 = \text{R}^2 = \text{R}^3 = \text{Me}$  **Fe5**;  $\text{R}^1 = \text{R}^2 = \text{Et}$ ,  $\text{R}^3 = \text{Me}$  **Fe6**], has been synthesized by the reaction of the corresponding compartmental ligand with two equivalents of  $\text{FeCl}_2 \cdot 4\text{H}_2\text{O}$ . The molecular structure of **Fe6** reveals an intramolecular  $\text{Fe} \cdots \text{Fe}$  separation of 10.152 Å, with pairs of **Fe6** assembling through intermolecular  $\text{OH} \cdots \text{Cl}$  hydrogen bonding interactions. On activation with MAO or MMAO, **Fe1** - **Fe6** exhibited both good thermal stability and very high activity for ethylene polymerization with the least sterically bulky **Fe1** the standout performer (up to  $2.43 \times 10^7 \text{ g} \cdot \text{mol}^{-1}(\text{Fe}) \cdot \text{h}^{-1}$  at 60 °C). Notably, **Fe1**/MAO showed almost double the activity of a structurally related mononuclear catalyst while the resultant polyethylene exhibited much higher molecular weight. In general, the polymeric materials are highly linear and have a tendency to display bimodal distributions that is influenced by the amount of co-catalyst employed. End-group analysis of the polymers generated using MMAO activation reveals chain ends composed of vinyl and saturated groups (propyl and isobutyl), while with MAO a preference for propyl end groups is observed.

## INTRODUCTION

The emergence of bis(imino)pyridine-iron complexes as highly active catalysts for the polymerization of ethylene at the end of the 1990's has been the driving force behind numerous follow-up studies.<sup>1</sup> In the main, these have focused on modifications to the bis(imino)pyridine supporting ligand and indeed progress in this field has been the subject of a number of reviews and book chapters.<sup>2</sup> Elsewhere, the incorporation of more than one polymerization-active iron center on the same ligand framework has emerged as an attractive target due to potential synergic effects caused by the close proximity of the active sites.<sup>3</sup> With regard to the supporting compartmental ligand, scaffolds based on linked bis(imino)pyridines have proved most effective with many of the resulting multinuclear iron complexes reported to display not only high activities but also performance characteristics that can be quite different to their mononuclear counterparts.<sup>4,5</sup> For example, the macrocyclic trinuclear 2,6-bis(imino)pyridine-iron complex **A** (Chart 1) exhibited a much longer lifetime than its mononuclear analogue and produced much higher molecular weight polyethylene with a unimodal distribution.<sup>6</sup> Similarly, the methylene-bridged bis(imino)pyridine complex **B** (Chart 1) produced polyethylenes with high molecular weight but with broad dispersities,<sup>7</sup> while the biphenyl-bridged bis(imino)pyridine complexes **C** (Chart 1) showed superior thermal stability and higher activities when compared to their mononuclear comparators.<sup>8</sup> In addition, Takeuchi's group reported the 'double-decker' complex **D** (Chart 1) which showed good activity at high operating temperatures and produced polyethylenes with narrow molecular weight distributions.<sup>9</sup>

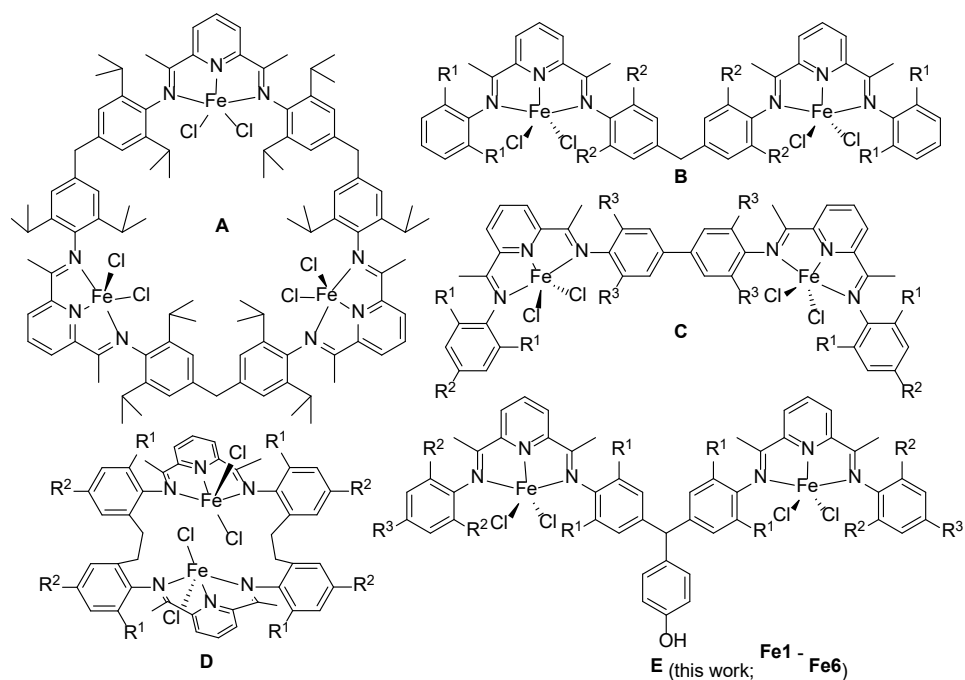


**Chart 1** Reported multinuclear bis(imino)pyridine-iron precatalysts, **A – D**, along with **E** to be developed in this work

In this report we are concerned with developing a series of diiron ethylene polymerization precatalysts of type **E** (Chart 1), in which the two metal centers are located within the *N,N,N* pockets of a methylene-bridged bis(imino)pyridine that has been additionally appended with a phenol group. We reasoned that the phenol moiety would be proton responsive during precatalyst activation and potentially affect the net charge of the active metal centers and in turn the polymerization performance.<sup>10-12</sup> Indeed, we have recently reported that the cobalt analogues of **E** display high activities for ethylene polymerization producing highly linear polyethylenes with high levels of vinyl chain ends.<sup>13</sup> Given the general tendency of bis(imino)pyridine-iron complexes to show higher activity than their cobalt analogues, we herein disclose our polymerization results for six examples of **E** in which the steric and electronic profile of the *N*-aryl groups within the compartmental ligand have been systematically varied. In addition, the effect of aluminoxane

co-catalyst, temperature, run time and pressure are explored and the resulting catalytic performances and polymer properties compared with **B** and **C** (Chart 1) as well as a mononuclear iron comparator. Full synthetic and characterization data is also presented for all the new complexes and ligands.

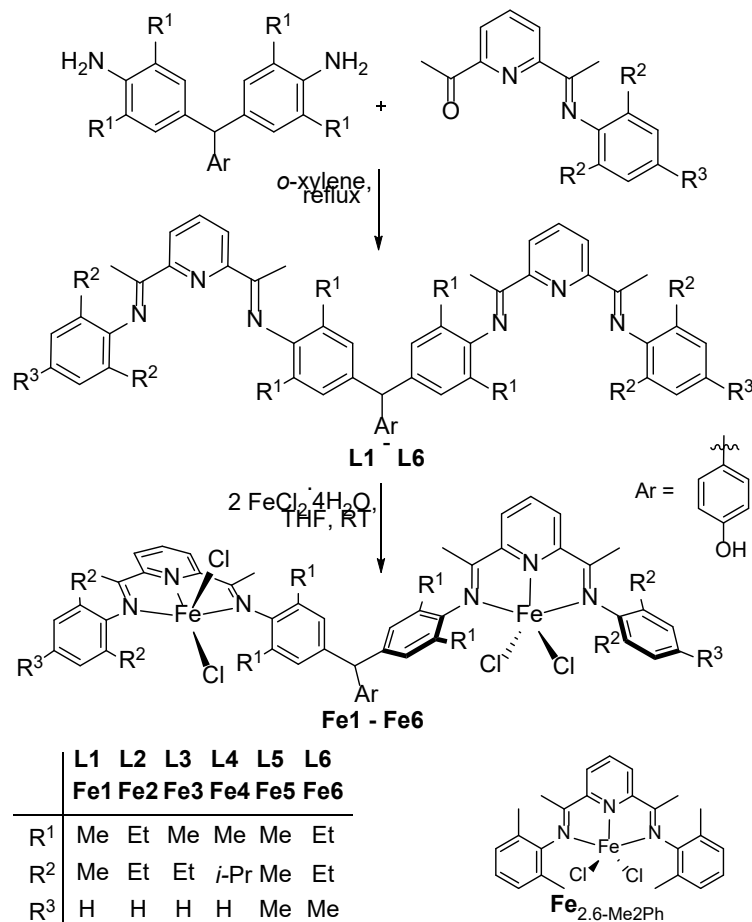
## RESULTS AND DISCUSSION

### Synthesis and characterization

The diiron(II) complexes,  $\text{CH}(\text{C}_6\text{H}_4\text{-4-OH})\{2'-(4\text{-C}_6\text{H}_2\text{-2,6-(R}^1\text{)}_2\text{N=CMe)}\text{-6'-(2'',6''-(R}^2\text{)}_2\text{-4-(R}^3\text{)C}_6\text{H}_2\text{N=CMe)}\text{C}_5\text{H}_3\text{N}\}_2\text{Fe}_2\text{Cl}_4$  [ $\text{R}^1 = \text{R}^2 = \text{Me}$ ,  $\text{R}^3 = \text{H}$  **Fe1**;  $\text{R}^1 = \text{R}^2 = \text{Et}$ ,  $\text{R}^3 = \text{H}$  **Fe2**;  $\text{R}^1 = \text{Me}$ ,  $\text{R}^2 = \text{Et}$ ,  $\text{R}^3 = \text{H}$  **Fe3**;  $\text{R}^1 = \text{Me}$ ,  $\text{R}^2 = i\text{-Pr}$ ,  $\text{R}^3 = \text{H}$  **Fe4**;  $\text{R}^1 = \text{R}^2 = \text{R}^3 = \text{Me}$  **Fe5**;  $\text{R}^1 = \text{R}^2 = \text{Et}$ ,  $\text{R}^3 = \text{Me}$  **Fe6**], have been prepared as green solids in good yield by treating the corresponding compartmental ligand, **L1 - L6**, with two molar equivalents of  $\text{FeCl}_2 \cdot 4\text{H}_2\text{O}$  in freshly distilled THF at room temperature (Scheme 1). All the ferrous complexes are air stable in the solid state but show some evidence for oxidation on prolonged standing in solution in the air. Each complex has been characterized by FT-IR spectroscopy, elemental analysis and in the case of **Fe6** by single crystal X-ray diffraction.

Compounds **L1 - L4** have been reported previously,<sup>13</sup> while  $\text{CH}(\text{C}_6\text{H}_4\text{-4-OH})\{2'-(4\text{-C}_6\text{H}_2\text{-2,6-(R}^1\text{)}_2\text{N=CMe)}\text{-6'-(2'',6''-(R}^2\text{)}_2\text{-4-(R}^3\text{)C}_6\text{H}_2\text{N=CMe)}\text{C}_5\text{H}_3\text{N}\}_2$  ( $\text{R}^1 = \text{R}^2 = \text{R}^3 = \text{Me}$  **L5**;  $\text{R}^1 = \text{R}^2 = \text{Et}$ ,  $\text{R}^3 = \text{Me}$  **L6**) are new and have been synthesized by reacting the corresponding diamine,  $\text{CH}(\text{C}_6\text{H}_4\text{-4-OH})(4\text{-C}_6\text{H}_2\text{-2,6-R}^1\text{)}_2\text{NH}_2$  ( $\text{R}^1 = \text{Me}$ ,  $\text{Et}$ ), with just over two equivalents of the appropriate 2-acetyl-6-aryliminopyridine, 2-(CMeO)-6- $\{(CMe=N(2,6-(R^2)_2-4-R^3C_6H_2)\}C_5H_3N$  ( $\text{R}^2 = \text{R}^3 = \text{Me}$ ;  $\text{R}^2 = \text{Et}$ ,  $\text{R}^3 = \text{Me}$ ), in

*ortho*-xylene at reflux (Scheme 1). Both **L5** and **L6** have been characterized by  $^1\text{H}/^{13}\text{C}$  NMR and FT-IR spectroscopy as well as by elemental analysis. Notably, the  $-\text{OH}$  resonance in their  $^1\text{H}$  NMR spectra, recorded in  $\text{DMSO}-d_6$ , could be observed around  $\delta$  9.23.



**Scheme 1** Synthetic route to bimetallic **Fe1 – Fe6**

Single crystals of **Fe6** suitable for the X-ray determination were grown by slow diffusion of diethyl ether into a dimethylformamide solution of the complex. A view of **Fe6** is shown in Figure 1; selected bond lengths and angles are collected in Table 1. The structure consists of two iron atoms that are each bound to three nitrogen donors belonging to **L6** and two chloride ligands to complete distorted trigonal bipyramidal geometries at each metal center. Within each *N,N,N* pocket, the central  $\text{Fe}-\text{N}_{\text{pyridine}}$  bond lengths of 2.127(4) Å [ $\text{Fe}(1)-\text{N}(2)$ ] and 2.093(4) Å [ $\text{Fe}(2)-\text{N}(5)$ ] are shorter

than the exterior Fe-N<sub>imine</sub> ones [Fe(1)-N(1) 2.248(5), Fe(1)-N(3) 2.250(4), Fe(2)-N(4) 2.200(4) and Fe(2)-N(6) 2.201(4)]; an observation that is common to many bis(imino)pyridine-iron complexes.<sup>1,14</sup> The sp<sup>3</sup>-hybridization of the bridging methylene unit [C(21)-C(20)-C(13) 112.5(4)°] leads to the two *N,N,N*-chelation planes [N(1)-N(2)-N(3) and N(4)-N(5)-N(6)] being inclined at an angle of 76.58° which in turn results in the iron centers being separated by a distance of 10.152 Å. The N-aryl rings are almost perpendicular to the adjacent pyridine rings with dihedral angles of 85.19° and 88.26° for Fe(1) and 76.79° and 83.38° for Fe(2). In addition, the presence of the OH functionality on the phenol unit results in neighboring molecules assembling *via* Cl<sup>1</sup>··HO intramolecular hydrogen bonding interactions (3.163 Å, see Figure 2).

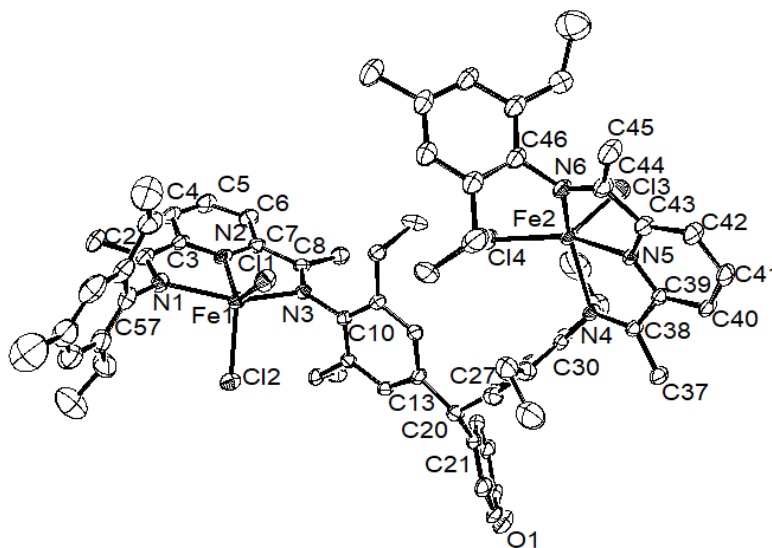


**Figure 1** ORTEP representation of **Fe6**. The thermal ellipsoids are shown at the 30% probability level while the hydrogen atoms and the positional disorder present in some ethyl groups, have been omitted for clarity.

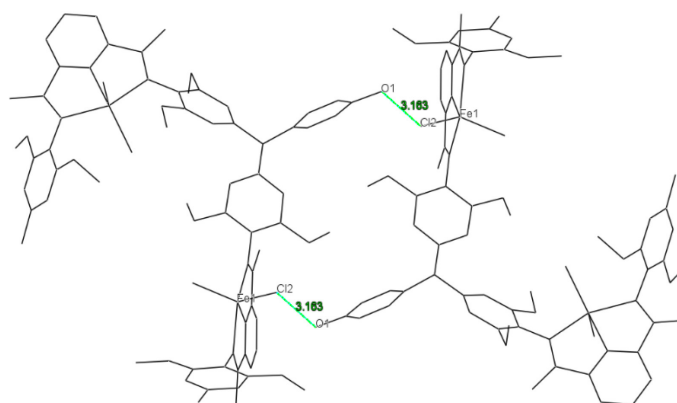


**Figure 2** Pairing of molecules of **Fe6** through intermolecular Cl $\cdots$ HO hydrogen-bonding

**Table 1** Selected bond lengths (Å) and angles (°) for **Fe6**

Bond Lengths (Å)			
Fe(1)-N(1)	2.248(5)	Fe(2)-N(6)	2.201(4)
Fe(1)-N(2)	2.127(4)	Fe(2)-N(5)	2.093(4)
Fe(1)-N(3)	2.250(4)	Fe(2)-N(4)	2.200(4)
N(1)-C(2)	1.283(6)	N(6)-C(46)	1.440(7)
N(1)-C(57)	1.433(6)	N(6)-C(44)	1.294(7)
N(2)-C(3)	1.343(6)	N(5)-C(43)	1.333(6)
N(2)-C(7)	1.329(7)	N(5)-C(39)	1.337(6)
N(3)-C(10)	1.438(6)	N(4)-C(38)	1.278(6)
N(3)-C(8)	1.275(6)	N(4)-C(30)	1.436(6)
Bond Angles (°)			
N(2)-Fe(1)-Cl(1)	128.22(13)	N(5)-Fe(2)-Cl(4)	154.36(13)
N(3)-Fe(1)-Cl(2)	98.99(11)	N(4)-Fe(2)-Cl(3)	101.16(13)
N(1)-Fe(1)-Cl(2)	98.39(13)	N(6)-Fe(2)-Cl(3)	103.32(13)
Cl(2)-Fe(1)-Cl(1)	108.88(6)	Cl(3)-Fe(2)-Cl(4)	113.31(6)
C(3)-N(2)-C(7)	121.4(5)	C(39)-N(5)-C(43)	121.3(4)
C(2)-N(1)-C(57)	120.3(5)	C(44)-N(6)-C(46)	120.3(5)
C(8)-N(3)-C(10)	121.7(4)	C(38)-N(4)-C(30)	121.5(4)
C(21)-C(20)-C(13)	112.5(4)	C(21)-C(20)-C(27)	114.7(4)

In comparison with the corresponding free ligand, the  $\nu(\text{C}=\text{N})_{\text{imine}}$  stretching frequencies in the IR spectra for **Fe1** - **Fe6**, are each shifted to lower wavenumber by *ca.* 20  $\text{cm}^{-1}$ , in agreement with coordination of all four imine nitrogen atoms. Their  $\nu(\text{O}-\text{H})_{\text{phenol}}$  absorptions fall around 3300  $\text{cm}^{-1}$  supportive of the hydrogen bonding observed in the crystal structure

of **Fe6**. Furthermore, the microanalytical data for all six complexes are consistent with each structure adopting a composition based on  $[(L)Fe_2Cl_4]$ .

### Ethylene polymerization

To explore the performance characteristics of **Fe1** – **Fe6** as precatalysts for ethylene polymerization, methylaluminoxane (MAO) and modified methylaluminoxane (MMAO, AlMeO:Al-*i*-BuO 3:1) were chosen as the co-catalysts to allow two parallel studies. Indeed, such aluminoxanes have shown themselves as among the most effective co-catalysts for activating mononuclear bis(imino)pyridine-iron(II) halide complexes and indeed differences in catalytic performance and polymer properties have been noted between the two activators.<sup>1,14</sup> To allow an optimization of the conditions, **Fe1** was selected as the test precatalyst in each study. The polymerizations were typically performed in toluene at 10 atm C<sub>2</sub>H<sub>4</sub> over 30 minute run times. All the polymers have been characterized by gel permeation chromatography (GPC) and differential scanning calorimetry (DSC). In addition, high temperature NMR spectroscopy was employed to examine the structural properties of selected polymer samples.

(a) *Catalytic evaluation of Fe1 – Fe6/MAO.* To determine the optimal conditions using MAO as co-catalyst, the effects of temperature, Al:Fe molar ratio, pressure and reaction time were all investigated with **Fe1** as the precatalyst; the results are collected in the Table 2.

Firstly, the effect of temperature was explored as it has been shown to have a significant effect on not only the polymerization activity of an iron catalyst but also the structure of the resultant polymer.<sup>15</sup> Hence, the polymerizations using **Fe1**/MAO were conducted at different temperatures between 40 and 80 °C with the Al:Fe molar ratio fixed at 1000 (runs 1 - 5, Table 2). The highest

activity of  $8.25 \times 10^6 \text{ g(PE)·mol}^{-1}(\text{Fe})\cdot\text{h}^{-1}$  was achieved at 60 °C and then steadily dropped as the temperature was raised before reaching a credible  $6.03 \times 10^6 \text{ g(PE)·mol}^{-1}(\text{Fe})\cdot\text{h}^{-1}$  at 80 °C, highlighting the good thermal stability of this catalyst. Similarly, the molecular weight ( $M_w$ ) of the polyethylene reached a maximum of  $207 \text{ kg·mol}^{-1}$  at 60 °C and then dramatically dropped as the temperature was raised further. All the polyethylenes possessed broad but unimodal distributions under these conditions ( $M_w/M_n = 9.73 - 17.7$ ), consistent with a uniform active species in the polymerization process (Figure 3).

**Table 2** Catalytic evaluation using **Fe1 – Fe6/MAO**<sup>a</sup>

Runs	Precat.	Al:Fe	T (°C)	t (min)	Mass of PE (g)	Activity <sup>b</sup>	$M_w^c$	$M_w/M_n^d$	$T_m$ (°C) <sup>e</sup>
1	<b>Fe1</b>	1000	40	30	7.90	3.95	163	14.3	136.3
2	<b>Fe1</b>	1000	50	30	13.5	6.75	166	16.1	134.6
3	<b>Fe1</b>	1000	60	30	16.5	8.25	207	17.7	133.6
4	<b>Fe1</b>	1000	70	30	12.3	6.15	108	12.8	132.8
5	<b>Fe1</b>	1000	80	30	12.1	6.05	99.5	9.73	132.6
6	<b>Fe1</b>	1500	60	30	19.0	9.50	172	13.6	134.1
7	<b>Fe1</b>	2000	60	30	21.0	10.5	160	10.7	131.7
8	<b>Fe1</b>	2250	60	30	22.2	11.1	152	19.5	131.5
9	<b>Fe1</b>	2500	60	30	25.1	12.6	121	14.5	131.7
10	<b>Fe1</b>	2750	60	30	23.7	11.9	94.8	14.9	130.6
11	<b>Fe1</b>	2500	60	5	7.46	22.4	37.3	7.80	128.5
12	<b>Fe1</b>	2500	60	15	24.3	24.3	97.4	10.6	130.8
13	<b>Fe1</b>	2500	60	45	26.7	8.90	187	15.5	131.9
14	<b>Fe1</b>	2500	60	60	27.0	6.75	178	18.4	131.3
15 <sup>f</sup>	<b>Fe1</b>	2500	60	30	0.61	0.31	105	14.3	131.0
16 <sup>g</sup>	<b>Fe1</b>	2500	60	30	11.7	5.85	133	20.2	130.4
17	<b>Fe2</b>	2500	60	30	14.5	7.25	125	20.0	129.2
18	<b>Fe3</b>	2500	60	30	15.2	7.60	90.4	28.9	130.1
19	<b>Fe4</b>	2500	60	30	13.1	6.55	127	29.0	132.1
20	<b>Fe5</b>	2500	60	30	21.6	10.8	84.9	18.3	131.3
21	<b>Fe6</b>	2500	60	30	13.8	6.90	92.1	30.5	129.7
22	<b>Fe</b> <sub>2,6-Me2Ph</sub>	2500	60	30	5.40	5.40	21.4	8.49	128.5
23	<b>B</b> <sub>2,6-Me2Ph</sub> <sup>h</sup>	2500	60	30	10.5	5.25	92.9	8.31	133.7

<sup>a</sup> Conditions: 2.0 μmol of precatalyst, 10 atm C<sub>2</sub>H<sub>4</sub>, toluene, total volume 100 mL;

<sup>b</sup> Activity:  $\times 10^6 \text{ g(PE)·mol}^{-1}(\text{Fe})\cdot\text{h}^{-1}$ ;

<sup>c</sup>  $M_w$  in  $\text{kg}\cdot\text{mol}^{-1}$ ;

<sup>d</sup>  $M_w$  and  $M_w/M_n$  determined by GPC;

<sup>e</sup> Determined by DSC;

<sup>f</sup> 1 atm  $\text{C}_2\text{H}_4$ ;

<sup>g</sup> 5 atm  $\text{C}_2\text{H}_4$ ;

<sup>h</sup> Binuclear iron complex **B** ( $\text{R}^1 = \text{R}^2 = \text{Me}$ ) (Chart 1).

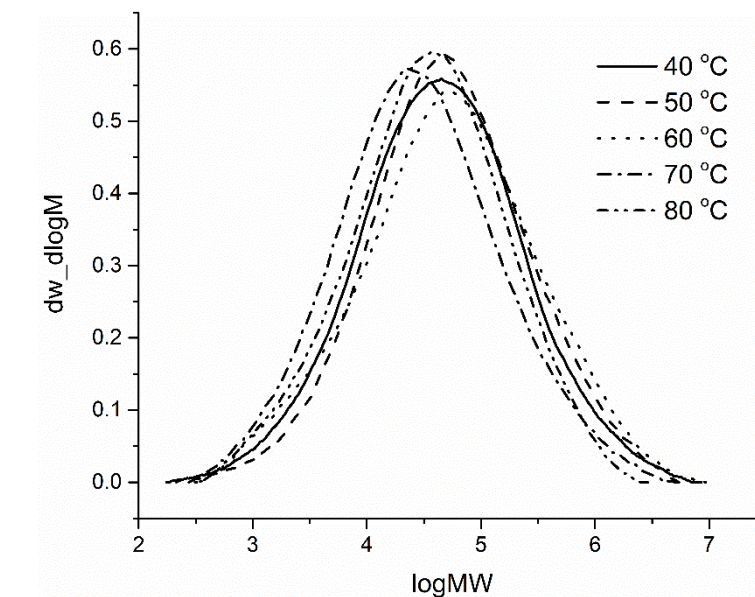


**Figure 3** GPC curves of the polyethylene obtained using **Fe1**/MAO at different temperatures (runs 1 – 5, Table 2)

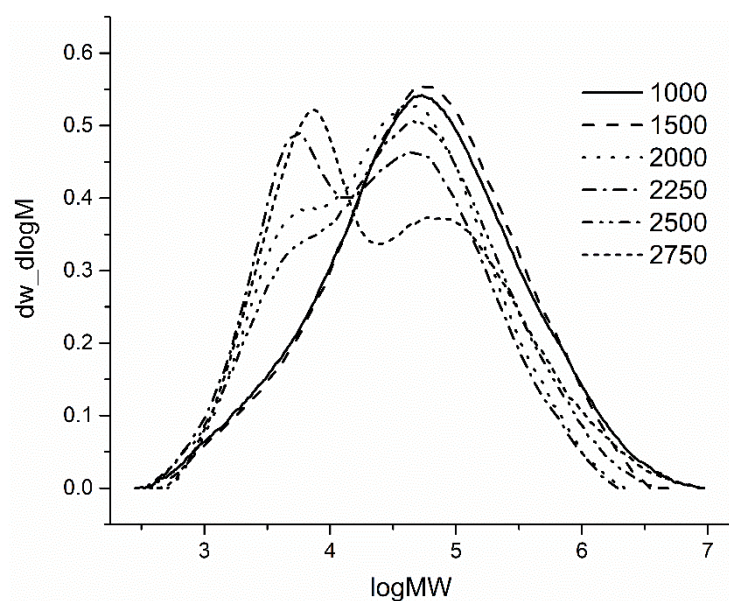


**Figure 4** GPC curves of the polyethylene produced using **Fe1**/MAO at different Al:Fe molar ratios (runs 3, 6 – 10, Table 2)

Secondly, with the temperature maintained at 60 °C, the molar ratio of **Fe1** to MAO was

progressively increased from 1000 to 2750 (runs 3, 6 – 10, Table 2). A peak in activity of  $12.6 \times 10^6$  g(PE)·mol<sup>-1</sup>(Fe)·h<sup>-1</sup> was achieved at a ratio of 2500 above which a slight decrease was noted. In terms of molecular weight, the  $M_w$  values were found to drop steadily from a maximum of 207 kg·mol<sup>-1</sup> at an Al:Fe ratio of 1000 to 94.8 kg·mol<sup>-1</sup> at 2750, in accord with more chain transfer to aluminum at higher molar ratios (Figure 4). Interestingly, unimodal distributions were only observed with lower amounts of MAO (Al:Fe = 1000, 1500), while bimodal distributions became more apparent at higher ratios (Figure 4). Notably, on raising the Al:Fe molar ratio from 2000 to 2750, the lower molecular weight peak gradually became the more intense of the two peaks in the distribution, consistent with chain transfer to aluminum becoming increasingly operative.<sup>1a</sup>

Thirdly, the effect of pressure was examined on the performance of **Fe1**/MAO (runs 9, 15, 16, Table 2). On reducing the ethylene pressure from 10 to 5 atm with the temperature kept at 60 °C and the Al:Fe molar ratio at 2500, the activity decreased from  $12.6$  to  $5.85 \times 10^6$  g(PE)·mol<sup>-1</sup>(Fe)·h<sup>-1</sup>. Similarly, with the pressure lowered to 1 atm the activity dropped even further to  $0.31 \times 10^6$  g(PE)·mol<sup>-1</sup>(Fe)·h<sup>-1</sup>. This pressure/activity correlation can be explained by the slower ethylene coordination and insertion rate at lower ethylene pressures.<sup>16</sup> On the other hand, no discernible trends could be identified in the molecular weight with the  $M_w$  values falling between 105 and 133 kg·mol<sup>-1</sup> across the three pressures.

Fourthly, by fixing the Al:Fe molar ratio at 2500, the temperature at 60 °C and the pressure at 10 atm C<sub>2</sub>H<sub>4</sub>, the catalytic lifetime of **Fe1**/MAO was evaluated by running the reactions over 5, 15, 30, 45 and 60 minutes (runs 9, 11 – 14, Table 2). Inspection of the data reveals an extremely high activity (up to  $2.24 \times 10^7$  g(PE)·mol<sup>-1</sup>(Fe)·h<sup>-1</sup>) was observed after 15 minutes followed by a steady

drop-off over longer reaction durations in accord with slow deactivation of the active species.<sup>17</sup> Nevertheless, even after 60 minutes a good activity of  $6.75 \times 10^6 \text{ g(PE)·mol}^{-1}(\text{Fe})\cdot\text{h}^{-1}$  was still achieved, highlighting the appreciable lifetime displayed by this catalyst. With regard to the molecular weight of the polymer, it was found to increase from 37.3 to 178  $\text{kg·mol}^{-1}$  over time, a similar upward trend was also noted for the molecular weight distribution ( $M_w/M_n$ : 7.8 to 18.4).

Finally, under the optimized conditions established for **Fe1**/MAO [Al:Fe ratio at 2500, the temperature at 60 °C, 10 atm C<sub>2</sub>H<sub>4</sub>], the catalytic performances of the remaining five precatalysts, **Fe2** - **Fe6**, were also evaluated; the results are discussed alongside that for **Fe1** (runs 9, 17 - 21, Table 2) and a structurally related mononuclear bis(imino)pyridine-iron complex (**Fe<sub>2,6-Me2Ph</sub>**, Scheme 1: run 22, Table 2). As a general point, **Fe1** - **Fe6** exhibited higher activity ( $6.90 - 12.6 \times 10^6 \text{ g(PE)·mol}^{-1}(\text{Fe})\cdot\text{h}^{-1}$ ) than that seen with **Fe<sub>2,6-Me2Ph</sub>** (Figure 5). In particular, the polymerization activity displayed by **Fe1** is more than double that observed for **Fe<sub>2,6-Me2Ph</sub>**, highlighting the apparent cooperative effects of the two iron centers on catalytic performance. In addition, the molecular weight of the polymers generated by **Fe1** - **Fe6** was much higher ( $M_w$  range: 84.9 - 125  $\text{kg·mol}^{-1}$ ) than that obtained using **Fe<sub>2,6-Me2Ph</sub>** ( $M_w = 21.4 \text{ kg·mol}^{-1}$ ), which would suggest that these binuclear catalysts favor chain propagation over chain transfer. With particular regard to the **Fe1** – **Fe6** series, the activity was found to fall in the order, **Fe1** (Me, Me, H) > **Fe5** (Me, Me, Me) > **Fe3** (Me, Et, H) > **Fe2** (Et, Et, H) > **Fe6** (Et, Et, Me) > **Fe4** (Me, *i*-Pr, H) implying that both steric and electronic effects are influential. In terms of steric properties, the more bulky catalysts led to the lowest polymerization activity with the most crowded **Fe4** the lowest; this finding can be attributed to the ethylene coordination and insertion steps being suppressed by the more sterically encumbered

environment.<sup>14a</sup> With regard to electronic effects, the presence of a *para*-methyl group is shown to exert a negative influence on the polymerization activity, which is borne out by comparison of **Fe1** with **Fe5** and **Fe2** with **Fe6**: **Fe1** ( $R^3 = H$ ) > **Fe5** ( $R^3 = Me$ ) and **Fe2** ( $R^3 = H$ ) > **Fe6** ( $R^3 = Me$ ). In terms of molecular weight, no clear trends could be identified with variations in the N-aryl group substitution pattern, with the  $M_w$  values falling in the range 90.4 – 125 kg·mol<sup>-1</sup>. As seen with **Fe1**/MAO at higher Al:Fe molar ratios, the GPC curves of the **Fe2** – **Fe6**/MAO again show broad bimodal distributions ( $M_w/M_n$  range: 8.49 - 30.5) (Figure 6).

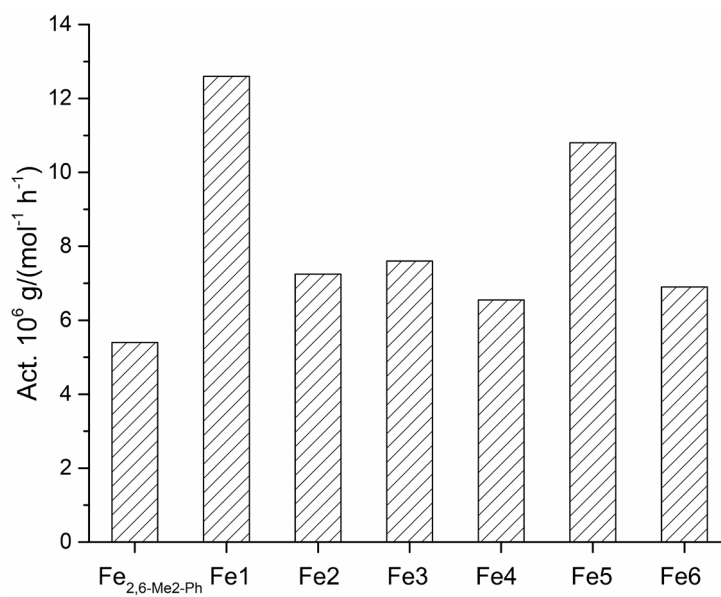


**Figure 5** Comparison of the polymerization activity displayed by **Fe1** – **Fe6** with **Fe<sub>2,6-Me2-Ph</sub>**; all precatalysts activated with MAO.

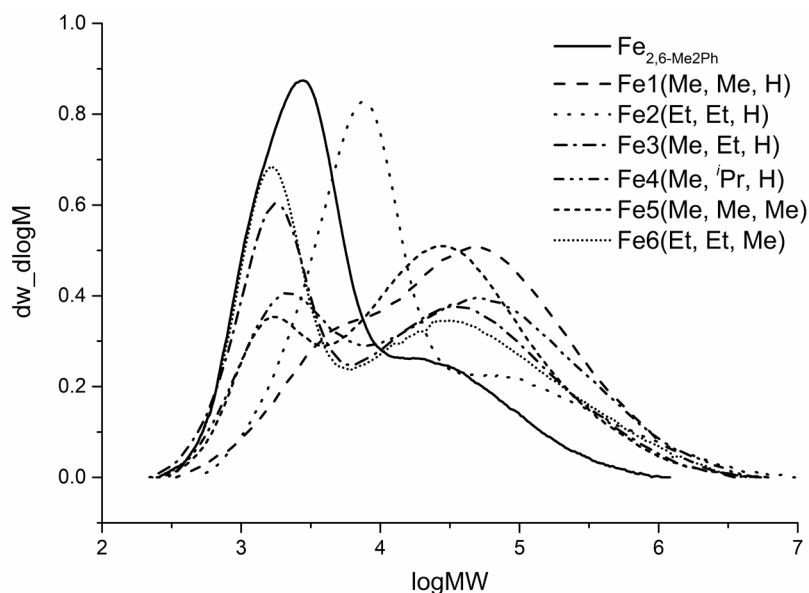


**Figure 6** The GPC curves of the polymers obtained using **Fe1 – Fe6** with MAO as co-catalyst; the data for **Fe<sub>2,6-Me<sub>2</sub>Ph</sub>**/MAO is also displayed

All the polymers generated using **Fe1 – Fe6**/MAO display melt temperatures between 128.5 and 136.3 °C which would suggest highly linear structures. To confirm this assertion and shed some light on the polymer end groups, a <sup>13</sup>C NMR spectrum was recorded on the polyethylene obtained using **Fe1**/MAO at 60 °C (run 9, Table 2). Examination of the spectrum reveals an intense peak at  $\delta$  29.4 which corresponds to the carbon atom belonging to the  $-(CH_2)_n-$  repeat unit of a linear polyethylene (Figure 7).<sup>18</sup> In addition, weaker peaks at  $\delta$  13.7 (a), 22.4 (b) and 31.7 (c) can be assigned to a propyl end group while no vinyl carbons could be detected in the downfield region. The <sup>1</sup>H NMR spectrum on the other hand, not only supports the <sup>13</sup>C NMR assignments but also reveals under close inspection a weak  $-CH=CH_2$  peak at  $\delta$  5.1 which would suggest a very low vinyl content in this high molecular weight polyethylene (Figure 7). Hence, these findings indicate that both chain transfer to aluminum and some  $\beta$ -H elimination/transfer are operative as termination pathways which in turn likely accounts for the bimodality observable in the GPC traces with large amounts of MAO.

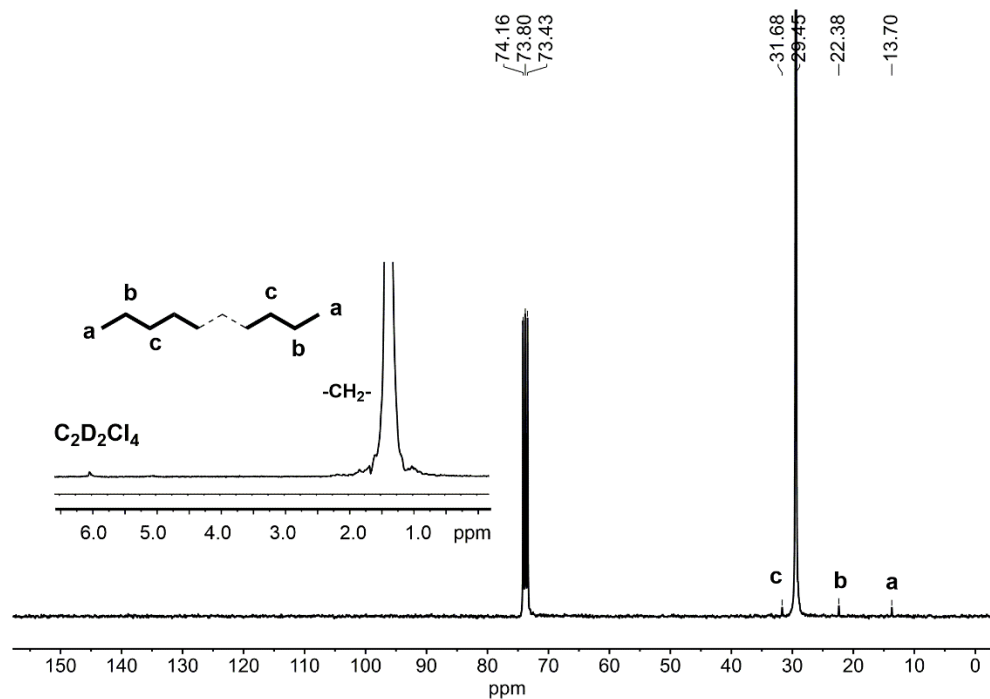


**Figure 7**  $^{13}\text{C}$  NMR spectrum of the polyethylene obtained using **Fe1**/MAO (run 9, Table 2), along with an insert of the  $^1\text{H}$  NMR spectrum; both spectra recorded at 100 °C in 1,1,2,2-tetrachloroethane- $d_2$

(b) *Catalytic evaluation of Fe1 – Fe6/MMAO.* To explore the effects of co-catalyst on the catalytic activity exhibited by **Fe1 – Fe6** as well as on the properties displayed by the resultant polymers, all six precatalysts were subject to an additional polymerization screen using MMAO; the results are gathered together in Table 3. Once again **Fe1** was used as the test precatalyst to allow an optimization of the reaction parameters.

With the Al:Fe ratio set at 1000, the temperature of the polymerization using **Fe1**/MMAO was varied between 40 and 80 °C with the optimal polymerization activity of  $1.08 \times 10^7 \text{g(PE)} \cdot \text{mol}^{-1}(\text{Fe}) \cdot \text{h}^{-1}$  attained at 60 °C (runs 1 - 5, Table 3). Further raising the temperature led to a gradual decrease in the activity with the catalyst notably still operating effectively at 80 °C ( $7.15 \times 10^6 \text{g(PE)} \cdot \text{mol}^{-1}(\text{Fe}) \cdot \text{h}^{-1}$ ); similar good thermal stability was also noted for **Fe1**/MAO. The

molecular weight ( $M_w$ ) of the polyethylene decreased sharply from 240 to 30.7 kg·mol<sup>-1</sup> on raising the temperature from 40 to 80 °C which can be attributed to the faster chain transfer rate and lower ethylene concentration at higher temperature.<sup>16,19</sup> This observation notably contrasts with that seen with the polymers obtained using **Fe1**/MAO in which a maximum in molecular weight (207 kg·mol<sup>-1</sup>) was seen at 60 °C.

**Table 3** Catalytic evaluation using **Fe1** – **Fe6**/MMAO<sup>a</sup>

Runs	Precat.	Al:Fe	T (°C)	t (min)	Mass of PE (g)	Activity <sup>b</sup>	$M_w$ <sup>c</sup>	$M_w/M_n$ <sup>d</sup>	$T_m$ (°C) <sup>e</sup>
1	<b>Fe1</b>	1000	40	30	8.83	5.89	240	15.0	135.9
2	<b>Fe1</b>	1000	50	30	9.21	6.14	81.1	16.9	131.5
3	<b>Fe1</b>	1000	60	30	16.2	10.8	71.9	11.4	132.1
4	<b>Fe1</b>	1000	70	30	13.6	9.07	55.5	7.43	132.1
5	<b>Fe1</b>	1000	80	30	10.7	7.13	30.7	5.54	131.5
6	<b>Fe1</b>	1500	60	30	18.7	12.5	61.1	15.2	131.6
7	<b>Fe1</b>	2000	60	30	19.5	13.0	53.6	17.3	129.2
8	<b>Fe1</b>	2500	60	30	22.5	15.0	46.9	12.4	131.3
9	<b>Fe1</b>	2750	60	30	24.7	16.5	39.3	16.8	129.0
10	<b>Fe1</b>	3000	60	30	18.6	12.4	29.8	11.0	129.7
12	<b>Fe1</b>	2750	60	5	5.76	23.0	9.22	9.57	124.0
13	<b>Fe1</b>	2750	60	15	17.0	22.7	19.3	8.55	128.1
14	<b>Fe1</b>	2750	60	45	25.1	11.2	43.6	18.4	128.3
15	<b>Fe1</b>	2750	60	60	25.2	8.40	45.3	21.2	128.0
16 <sup>f</sup>	<b>Fe1</b>	2750	60	30	0.49	0.33	16.6	11.9	127.3
17 <sup>g</sup>	<b>Fe1</b>	2750	60	30	13.0	8.67	29.7	14.3	129.3
18	<b>Fe2</b>	2750	60	30	15.8	10.5	49.1	25.8	127.3
19	<b>Fe3</b>	2750	60	30	16.1	10.7	25.0	20.9	127.3
20	<b>Fe4</b>	2750	60	30	14.0	9.33	76.2	33.3	129.4
20	<b>Fe5</b>	2750	60	30	17.6	11.7	34.4	13.5	128.6
21	<b>Fe6</b>	2750	60	30	14.3	9.53	101	26.2	131.9
22	<b>Fe</b> <sub>2,6-Me2Ph</sub>	2750	60	30	9.70	12.9	40.6	12.3	129.1
23	<b>B</b> <sub>2,6-Me2Ph</sub> <sup>h</sup>	2750	60	30	19.9	13.2	95.7	19.8	129.8

<sup>a</sup> Conditions: 1.5 μmol of precatalyst, 10 atm C<sub>2</sub>H<sub>4</sub>, toluene, total volume 100 mL;

<sup>b</sup> Activity: × 10<sup>6</sup> g(PE)·mol<sup>-1</sup>(Fe)·h<sup>-1</sup>;

<sup>c</sup>  $M_w$  in kg·mol<sup>-1</sup>;

<sup>d</sup>  $M_w$  and  $M_w/M_n$  determined by GPC;

<sup>e</sup> Determined by DSC;

<sup>f</sup> 1 atm C<sub>2</sub>H<sub>4</sub>;

<sup>g</sup> 5 atm C<sub>2</sub>H<sub>4</sub>;

<sup>h</sup> Binuclear iron complex **B** (R<sup>1</sup> = R<sup>2</sup> = Me) (Chart 1).

On varying the Al:Fe ratio from 1000 to 3000 with the temperature maintained at 60 °C, the highest activity for **Fe1**/MMAO of  $1.64 \times 10^7$  g(PE)·mol<sup>-1</sup>(Fe)·h<sup>-1</sup> was achieved with a ratio of 2750 (*c.f.* 2500 with MAO). The molecular weight of the polyethylene decreased gradually from 71.9 to 29.8 kg·mol<sup>-1</sup> on upping the ratio of Al:Fe, in line with increased chain transfer to aluminum with larger amounts of MMAO. As with the **Fe1**/MAO study, the GPC traces showed a bimodal distribution at higher molar ratios (Al:Fe > 1000), which suggests two different termination pathways are operational (Figure 8). Indeed, as previously observed, the lower molecular weight peak became the major peak with higher amounts of MMAO.<sup>16</sup>

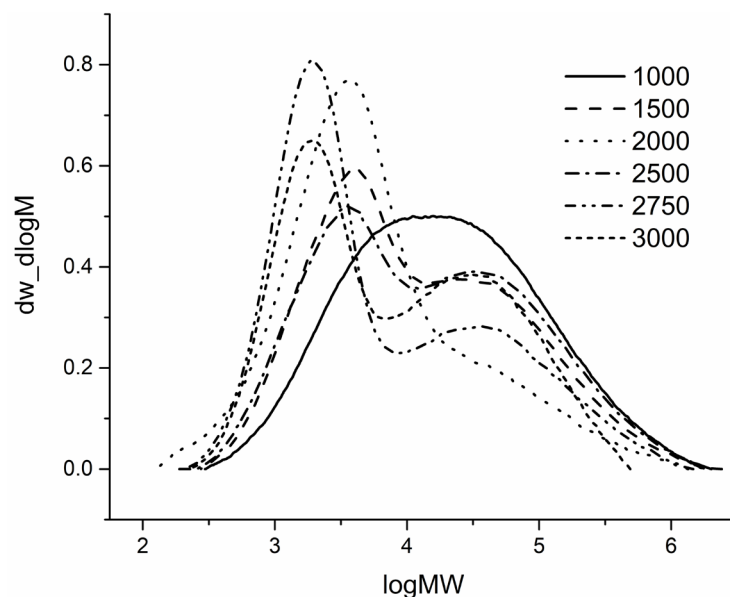


**Figure 8** GPC curves of the polyethylene produced using **Fe1**/MMAO at different Al:Fe molar ratios (runs 3, 6 - 10, Table 3)

The performance of **Fe1**/MMAO over time was also investigated by performing the polymerization at intervals between 5 and 60 minutes with the Al:Fe molar ratio fixed at 2750 (runs 9, 12 - 15, Table 3). Unlike with **Fe1**/MAO, the highest productivity of  $2.30 \times 10^7$  g(PE)·mol<sup>-1</sup>(Fe)·h<sup>-1</sup> was achieved after 5 minutes (*c.f.* 15 minutes for **Fe1**/MAO), suggesting the

induction period can be significantly reduced when using MMAO as co-catalyst. Even so, the activity gradually decreased over longer reaction times with the onset of catalyst deactivation.<sup>17</sup> However, despite this deactivation, the catalytic activity after 60 minutes remained high ( $8.40 \times 10^6$  g(PE)·mol<sup>-1</sup>(Fe)·h<sup>-1</sup>), once again highlighting the long lifetime of these bimetallic catalysts. As would be expected, the molecular weight gradually increased from 9.22 to 45.3 kg·mol<sup>-1</sup> over the course of the 60 minutes while the molecular weight distribution became broader ( $M_w/M_n$ : from 9.57 to 21.2).

The ethylene pressure also had a striking effect on the catalytic performance of **Fe1**/MMAO, which is similar to the results obtained using **Fe1**/MAO. On lowering the pressure from 10 to 1 atm (runs 9, 16, 17; Table 3), the polymerization activity significantly decreased from 16.5 to  $0.33 \times 10^6$  g(PE)·mol<sup>-1</sup>(Fe)·h<sup>-1</sup>. By contrast to that seen using **Fe1**/MAO, a downward trend in the molecular weight of the polyethylene is discernible in this case as the pressure was lowered.

Based on the optimized conditions determined using **Fe1**/MMAO [*viz.*, Al:Fe ratio at 2750, temperature at 60 °C, 10 atm C<sub>2</sub>H<sub>4</sub>], the performance of **Fe2** - **Fe6** as ethylene polymerization precatalysts was also assessed (runs 18 - 22, Table 3). Comparison of these data with that obtained for **Fe1**, reveals the catalytic activities for all six precatalysts fall in the order: **Fe1** (Me, Me, H) > **Fe5** (Me, Me, Me) > **Fe3** (Me, Et, H) > **Fe2** (Et, Et, H) > **Fe6** (Et, Et, Me) > **Fe4** (Me, *i*-Pr, H). Indeed, this order is similar to that found with MAO with both steric and electronic factors within the compartmental ligand influential. Once again, the least sterically bulky **Fe1** is the most active and, when compared with the results obtained involving MAO activation, **Fe1**/MMAO is the more productive [ $16.6 \times 10^6$  g(PE)·mol<sup>-1</sup>(Fe)·h<sup>-1</sup> vs.  $12.6 \times 10^6$  g(PE)·mol<sup>-1</sup>(Fe)·h<sup>-1</sup> for **Fe1**/MAO].

Conversely, the most bulky system, **Fe4**, is the least active precatalyst but forms the polymer of the highest molecular weight ( $M_w = 76.2 \text{ kg mol}^{-1}$ ) though less than that obtained with MAO ( $M_w = 127 \text{ kg mol}^{-1}$  using **Fe4**/MAO); such a finding can be accredited to the bulkier substituent impeding chain transfer leading to more effective propagation.<sup>20</sup> When compared with **Fe**<sub>2,6-Me<sub>2</sub>Ph</sub>, only **Fe1** exhibited higher activity while **Fe2** - **Fe6** were slightly less productive, results that differ from those observed using MAO (Figure 9). As seen with the polymers formed using **Fe1** – **Fe6**/MAO, all the polyethylenes in this MMAO study possessed bimodal distributions as opposed to a unimodal one observed using **Fe**<sub>2,6-Me<sub>2</sub>Ph</sub>/MMAO (Figure 10).

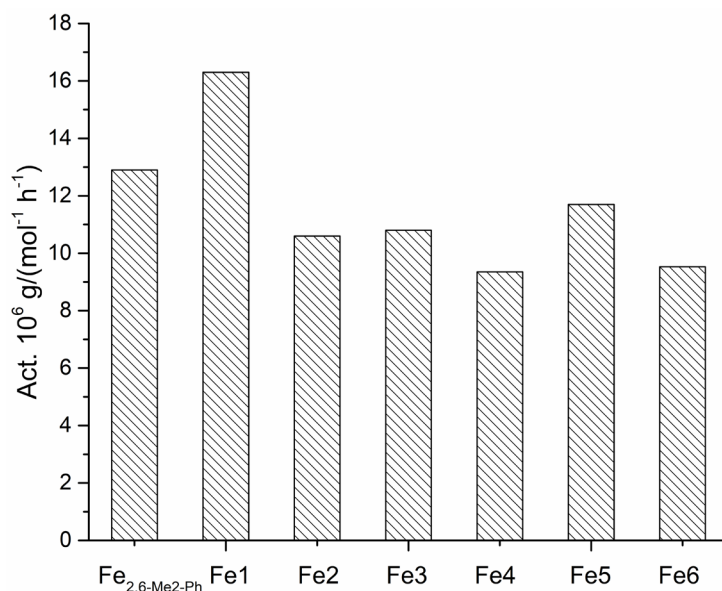


**Figure 9** Comparison of the activity of **Fe1** – **Fe6** with **Fe**<sub>2,6-Me<sub>2</sub>Ph</sub>; all precatalysts activated with MMAO

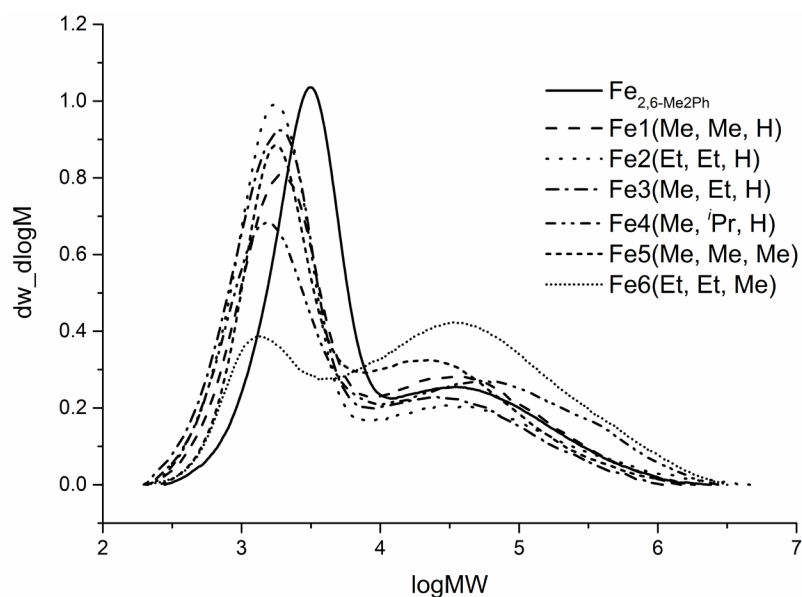


**Figure 10** GPC curves of the polymers obtained using **Fe1** – **Fe6**/MMAO along with that for **Fe<sub>2,6-Me<sub>2</sub>Ph</sub>**/MMAO

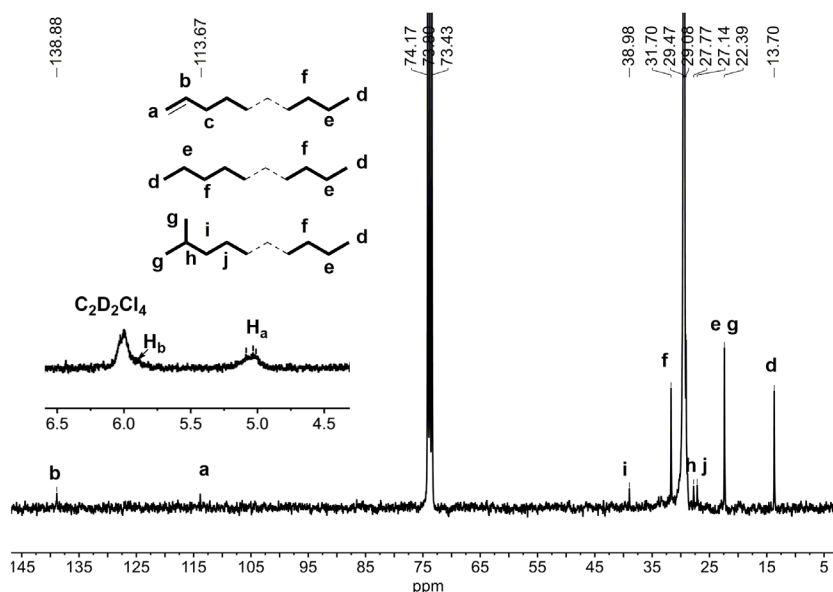


**Figure 11**  $^{13}\text{C}$  NMR spectrum of the polyethylene obtained using **Fe1**/MMAO (run 9, Table 3), along with an insert of the  $^1\text{H}$  NMR spectrum; both spectra recorded at 100 °C in 1,1,2,2-tetrachloroethane- $d_2$

To gain information as to the structural properties of the polyethylene and to ascertain any influence of the co-catalyst on this structure, the polymeric material obtained using **Fe1**/MMAO at 60 °C (run 9, Table 3) was selected as a representative example and characterized by high

temperature  $^1\text{H}$  and  $^{13}\text{C}$  NMR spectroscopy. As seen with the MAO study, the polymer is highly linear as evidenced by the intense signal at  $\delta$  29.5 in the  $^{13}\text{C}$  NMR spectrum (Figure 11). This observation is further supported by the  $T_m$  value of 129.0 °C which is typical of a highly linear polyethylene and indeed compares favorably to the values obtained for other samples in this MMAO study. In the  $^1\text{H}$  NMR spectrum signals at  $\delta$  5.0 ( $\text{H}_a$ ) and 5.9 ( $\text{H}_b$ ) are characteristic of a vinyl ( $\text{CH}=\text{CH}_2$ ) end group (Figure 11), which is backed up by the presence of downfield vinylic carbon resonances (a and b) in the  $^{13}\text{C}$  NMR spectrum. In addition, the upfield peaks at  $\delta$  13.7 (d), 22.4 (e) and 31.7 (f) can be ascribed to a propyl end group,<sup>18</sup> while the even weaker resonances at  $\delta$  27.8 (j), 29.1 (h) and 39.0 (i) can be assigned to an isobutyl end-group.<sup>21</sup> These variations in chain ends lends further support to  $\beta$ -H elimination (or transfer to monomer) and chain transfer to aluminum being operative.<sup>14b,18,22</sup> The first of these accounts for the formation of the vinyl chain end while the presence of an isobutyl group indicates that chain transfer to  $\text{Al}(i\text{-Bu}_3)$  and its derivatives present in MMAO can also occur.<sup>21, 23</sup> It is unclear why with MAO the termination pathway is biased towards chain transfer to aluminum but it could be due to the increased content of trimethylaluminum present in commercial MAO solutions. Nevertheless, it would seem probable that these two termination routes (as with the MAO study) account for the bimodal distribution seen in the GPC curves although the presence of two dissimilar iron active sites cannot be ruled out.

To allow for a comparison of the catalytic performance of **Fe1** with the previously reported diiron precatalysts **B**<sub>2,6-Me<sub>2</sub>Ph</sub> and **C**<sub>2,6-Me<sub>2</sub>Ph</sub>, Chart 2 lists selected molecular weight, dispersity, activity as well as optimal operating temperature data. With respect to methylene-bridged **B**<sub>2,6-Me<sub>2</sub>Ph</sub>, precatalyst **Fe1**, which differs only in the appended phenol group, showed enhanced thermal

stability as well as higher activity for ethylene polymerization. We propose that this improved performance can be accredited, in part, to the OH group undergoing reaction with the aluminoxane co-catalyst resulting in a change in net charge at the two active sites.<sup>10</sup> On the other hand, when compared with biphenyl-bridged  $C_{2,6-Me_2Ph}$ , **Fe1** showed higher activity at 60 °C. It is noteworthy that mononuclear bis(imino)pyridine-iron catalysts are known to suffer from deactivation issues and short lifetimes at higher temperatures and indeed much effort has been dedicated to try and overcome these limitations.<sup>14a,24</sup> Notably, **Fe1** reaches its optimal performance at 60 °C and, what is more, maintains this high activity even after one hour. Furthermore, **Fe1** has been shown to operate effectively even at 80 °C.

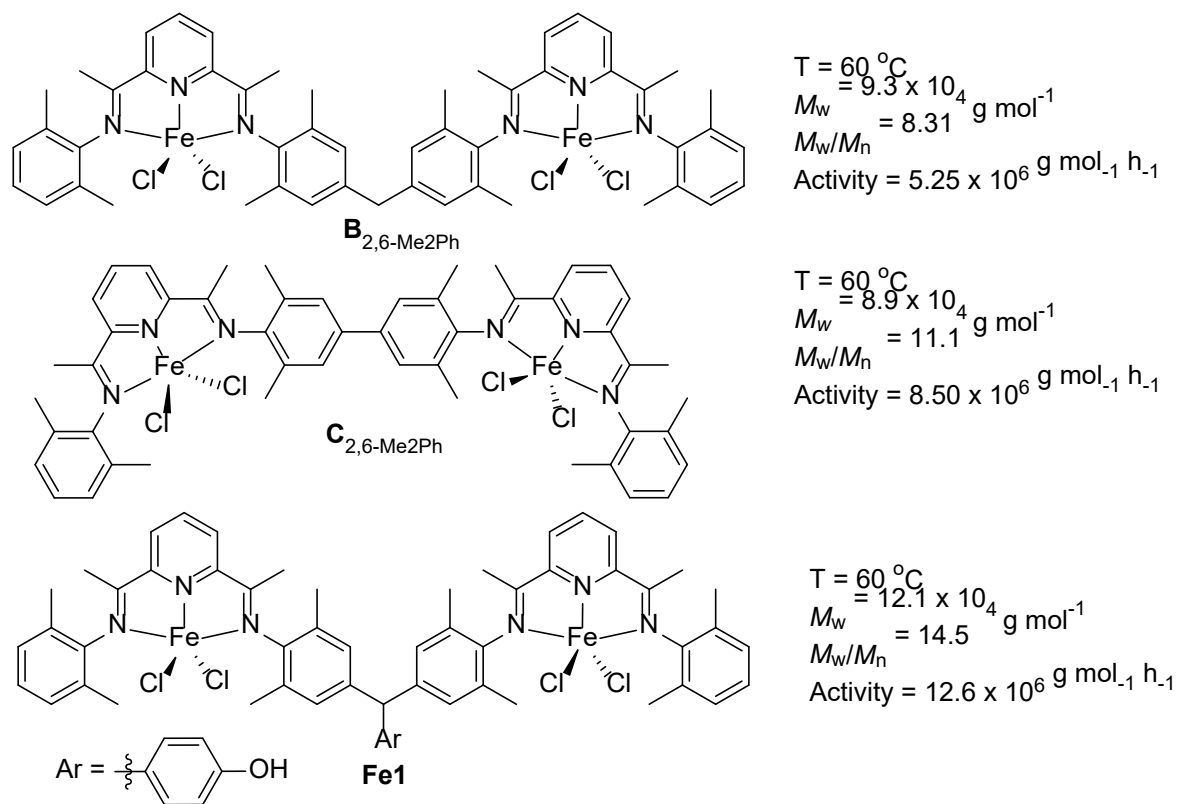


**Chart 2** Comparative performance data of **Fe1** with related binuclear iron precatalysts; MAO used as co-catalyst in each case

## CONCLUSIONS

The methylene-bridged bimetallic bis(imino)pyridine-iron complexes **Fe1** – **Fe6**, each substituted with a phenol group, have been successfully synthesized and characterized by IR spectroscopy and elemental analysis. The molecular structure of **Fe6** was confirmed by single crystal X-ray diffraction. On activation with MAO or MMAO, **Fe1** – **Fe6** displayed high activities for ethylene polymerization with the least sterically encumbered **Fe1** the most active and capable of operating effectively at temperatures up to 80 °C. Of particular note, **Fe1**/MAO showed more than double the activity displayed by mononuclear **Fe<sub>2,6</sub>-Me<sub>2</sub>Ph**, while the polyethylene possessed much higher molecular weight. Furthermore, the presence of the phenol unit on the ligand manifold of the bimetallic precatalyst has been shown to be beneficial to not only the thermal stability of the active catalyst but also the productivity. All the polymers are highly linear with bimodality a common feature of their distributions. Analysis of the polymer end groups obtained using MMAO reveals chain ends based on vinyl, propyl and isobutyl while with MAO propyl ends were identified as the major type, findings that highlight the competition in termination pathways that can operate in these polymerizations.

## EXPERIMENTAL SECTION

**General Considerations:** All manipulations involving air and moisture sensitive compounds were carried out under a nitrogen atmosphere using standard Schlenk techniques. Toluene was refluxed over sodium and distilled under nitrogen prior to use. Methylaluminoxane (MAO, 1.46 M solution in toluene) and modified methylaluminoxane (MMAO, 2.00 M in n-heptane) were purchased from

Akzo Nobel Corp. High purity ethylene was purchased from Beijing Yansan Petrochemical Co. and used as received. Other reagents were purchased from Aldrich, Acros or local suppliers. NMR spectra for the ligands were recorded on a Bruker DMX 400 MHz instrument at ambient temperature using TMS as an internal standard, while the NMR spectra of the polyethylenes were recorded on a Bruker DMX 300 MHz instrument at 100 °C in 1,1,2,2-tetrachloroethane-*d*<sub>2</sub> with TMS as an internal standard. IR spectra were recorded on a Perkin-Elmer System 2000 FT-IR spectrometer while elemental analyses were performed using a Flash EA 1112 micro-analyzer. Molecular weights and molecular weight distributions ( $M_w/M_n$ ) of the polyethylenes were determined using PL-GPC220 instrument at 150 °C with 1,2,4-trichlorobenzene as solvent. The melt temperatures of the polyethylenes were measured from the fourth scanning run on a Perkin-Elmer TA-Q2000 differential scanning calorimeter (DSC) under a nitrogen atmosphere. In the procedure, a sample of about 5.0 mg was heated to 160 °C at a rate of 20 °C min<sup>-1</sup> and maintained for 2 min at 160 °C to remove the thermal history and then cooled at a rate of 20 °C min<sup>-1</sup> to 20 °C. Ligands **L1** – **L4** were prepared as reported in the literature.<sup>13</sup> Compounds CH(C<sub>6</sub>H<sub>4</sub>-4-OH)(4-C<sub>6</sub>H<sub>2</sub>-2,6-R<sup>1</sup><sub>2</sub>NH<sub>2</sub>)<sub>2</sub> (R<sup>1</sup> = Me, Et) and 2-(CMeO)-6-{(CMe=N(2,6-R<sup>2</sup><sub>2</sub>-4-R<sup>3</sup>C<sub>6</sub>H<sub>2</sub>)}C<sub>5</sub>H<sub>3</sub>N (R<sup>2</sup> = R<sup>3</sup> = Me; R<sup>2</sup> = Et, R<sup>3</sup> = Me) were prepared according to literature procedures.<sup>25</sup> Complex **B**<sub>2,6-Me<sub>2</sub>Ph</sub> was prepared according to the literature procedure.<sup>7</sup>

**Synthesis of L5.** A catalytic amount of *p*-toluenesulfonic acid (*ca.* 0.15 g) was added to a solution of 2-(CMeO)-6-{(CMe=N(2,4,6-Me<sub>3</sub>C<sub>6</sub>H<sub>2</sub>)}C<sub>5</sub>H<sub>3</sub>N (2.80 g, 10.0 mmol) and CH(C<sub>6</sub>H<sub>4</sub>-4-OH)(4-C<sub>6</sub>H<sub>2</sub>-2,6-Me<sub>2</sub>NH<sub>2</sub>)<sub>2</sub> (1.40 g, 4.0 mmol) in *o*-xylene (100 mL) and the resulting mixture stirred

and heated to reflux for 12 h. On cooling to room temperature, the solvent was removed by rotary evaporation and the residue purified by column chromatography with petroleum ether/ethyl acetate (12:1) and a few drops of triethylamine as eluent affording **L5** as a yellow solid (0.60 g, 17%). <sup>1</sup>H NMR (400 MHz, CDCl<sub>3</sub>): δ 8.49 (d, *J* = 7.6 Hz, 4H, Py-*H*), 7.92 (t, *J* = 8.0 Hz, 2H, Py-*H*), 7.00 (d, *J* = 8.0 Hz, 2H, Ph-*H*), 6.92 (s, 4H, Ar-*H*), 6.89 (d, *J* = 6.0 Hz, 4H, Ar-*H*), 6.63 (d, *J* = 8.7 Hz, 2H, Ph-*H*), 5.39 (s, 1H, (Ar)<sub>2</sub>-CH-Ph), 2.31 (d, *J* = 7.6 Hz, 12H, -CH<sub>3</sub>), 2.26 (s, 6H, -CH<sub>3</sub>), 2.04 (s, 24H, -CH<sub>3</sub>). <sup>1</sup>H NMR (400 MHz, DMSO-*d*<sub>6</sub>): δ 9.25 (s, 1H, -OH); 8.44 (d, *J* = 8.0 Hz, 4H, Py-*H*), 8.10 (t, *J* = 8.0 Hz, 2H, Py-*H*), 6.98 (d, *J* = 8.0 Hz, 2H, Ph-*H*), 6.90-6.85 (s, 8H, Ar-*H*), 6.72 (d, *J* = 8.0 Hz, 2H, Ph-*H*), 5.32 (s, 1H, (Ar)<sub>2</sub>-CH-Ph), 2.26-2.16 (m, 18H, -N=CCH<sub>3</sub> and -CH<sub>3</sub>), 2.04 (s, 24H, -CH<sub>3</sub>). <sup>13</sup>C NMR (100 MHz, CDCl<sub>3</sub>): δ 168.2, 167.6, 155.4, 155.2, 154.6, 146.6, 146.3, 139.7, 137.0, 136.7, 132.4, 130.6, 129.2, 128.7, 125.5, 125.4, 122.5, 122.4, 115.3, 55.3, 46.0, 20.9, 18.3, 18.0, 16.9, 16.6, 11.0. FT-IR (KBr, cm<sup>-1</sup>): 2963 (w), 2916 (m), 2856 (w), 1640 (s, ν<sub>C=N</sub>), 1614 (w), 1571 (w), 1511 (m), 1474 (s), 1446 (m), 1363 (s), 1323 (w), 1295 (w), 1256 (m), 1212 (s), 1170 (w), 1145 (s), 1120 (m), 1077 (w), 1022 (m), 967 (w), 883 (w), 851 (m), 818 (s), 792 (m), 738 (m), 668 (w). Anal. Calcd. for C<sub>59</sub>H<sub>62</sub>N<sub>6</sub>O (954.59): C, 81.34; H, 7.17; N, 9.65. Found: C, 81.30; H, 6.99; N, 9.29%.

**Synthesis of L6.** Using the same procedure described for the synthesis of **L5**, but using as CH(C<sub>6</sub>H<sub>4</sub>-4-OH)(4-C<sub>6</sub>H<sub>2</sub>-2,6-Et<sub>2</sub>NH<sub>2</sub>)<sub>2</sub> as the diamine and 2-(CMeO)-6-((CMe=N(2,6-Et<sub>2</sub>-4-MeC<sub>6</sub>H<sub>2</sub>))C<sub>5</sub>H<sub>3</sub>N as the 2-acetyl-6-aryliminopyridine, **L6** was isolated as a yellow solid (0.57 g, 14%). <sup>1</sup>H NMR (400 MHz, CDCl<sub>3</sub>): δ 8.48 (d, *J* = 7.6 Hz, 4H, Py-*H*), 7.92 (t, *J* = 8.0 Hz, 2H, Py-*H*), 7.03 (d, *J* = 4.4 Hz, 2H, Ph-*H*), 6.95 (s, 6H, Ar-*H*), 6.91 (s,

2H, Ar-H), 6.64 (d,  $J = 8.4$  Hz, 2H, Ph-H), 5.45 (s, 1H, (Ar)<sub>2</sub>-CH-Ph), 2.44-2.27 (m, 34H, -CH<sub>2</sub>CH<sub>3</sub> and CH<sub>3</sub>), 1.17-1.07 (m, 24H, -CH<sub>3</sub>). <sup>1</sup>H NMR (400 MHz, DMSO-*d*<sub>6</sub>):  $\delta$  9.23 (s, 1H, -OH), 8.42 (d,  $J = 8.0$  Hz, 4H, Py-H), 8.10 (t,  $J = 8.0$  Hz, 2H, Py-H), 7.00 (d,  $J = 12.0$  Hz, 2H, Ph-H), 6.92-6.90 (m, 8H, Ar-H), 6.72 (d,  $J = 8.0$  Hz, 2H, Ph-H), 5.39 (s, 1H, (Ar)<sub>2</sub>-CH-Ph), 2.30-2.17 (m, 34H, -CH<sub>2</sub>CH<sub>3</sub> and CH<sub>3</sub>), 1.17-0.99 (m, 24H, -CH<sub>3</sub>). <sup>13</sup>C NMR (100 MHz, CDCl<sub>3</sub>):  $\delta$  167.8, 167.3, 155.4, 155.2, 154.2, 145.6, 145.4, 139.9, 137.3, 137.0, 132.6, 131.2, 131.1, 130.6, 127.4, 127.3, 126.8, 122.3, 115.2, 55.6, 46.0, 24.8, 24.7, 21.1, 17.2, 16.9, 14.0. FT-IR (KBr, cm<sup>-1</sup>): 2964 (m), 2929 (w), 2870 (w), 1640 (s,  $\nu_{C=N}$ ), 1571 (w), 1511 (m), 1457 (s), 1363 (s), 1324 (w), 1244 (m), 1207 (s), 1170 (w), 1144 (w), 1120 (s), 1076 (m), 994 (w), 884 (w), 866 (w), 857 (m), 816 (s), 738 (m), 668 (w). Anal. Calcd. for C<sub>67</sub>H<sub>78</sub>N<sub>6</sub>O (983.40): C, 81.83; H, 8.00; N, 8.55. Found: C, 81.50; H, 8.10; N, 8.27%.

**Synthesis of Fe1.** L1 (0.17 g, 0.20 mmol) and FeCl<sub>2</sub>·4H<sub>2</sub>O (0.080 g, 0.40 mmol) were combined in a Schlenk tube, previously purged three times with argon, and charged with THF (10 mL). The reaction mixture was then stirred at room temperature overnight. The resulting precipitate was filtered, washed with diethyl ether and dried under reduced pressure to give Fe1 as a green solid (0.18 g, 82%). FT-IR (KBr, cm<sup>-1</sup>): 3356 (w,  $\nu_{OH}$ ), 2915 (w), 2851 (w), 1689 (w), 1619 (m,  $\nu_{C=N}$ ), 1589 (s), 1510 (m), 1473 (s), 1443 (m), 1371 (m), 1264 (s), 1213 (s), 1171 (w), 1102 (w), 1029 (m), 989 (w), 887 (w), 830 (s), 771 (s), 736 (w), 662 (w), 593 (w), 528 (w), 421 (w). Anal. Calcd. for C<sub>57</sub>H<sub>58</sub>Cl<sub>4</sub>Fe<sub>2</sub>N<sub>6</sub>O (1094.21): C, 62.43; H, 5.33; N, 7.66. Found: C, 62.24; H, 5.71; N, 7.35%.

**Synthesis of Fe2.** Using the same procedure as described for the synthesis of Fe1 with L2 as the ligand, Fe2 was obtained as a green powder (0.16 g, 66%). FT-IR (KBr, cm<sup>-1</sup>): 3332 (w,  $\nu_{OH}$ ), 2969 (w), 2932 (w), 2875 (w), 1689 (w), 1618 (m,  $\nu_{C=N}$ ), 1587 (s), 1511 (m), 1461 (s), 1443 (m), 1371

(m), 1340 (w), 1264 (s), 1211 (s), 1171 (w), 1103 (w), 1028 (m), 988 (w), 887 (w), 835 (s), 810 (s), 770 (m), 738 (w), 674 (w), 592 (w), 528 (w), 477 (w), 439 (w), 421 (w). Anal. Calcd. for  $C_{65}H_{74}Cl_4Fe_2N_6O$  (1206.34): C, 64.58; H, 6.17; N, 6.95. Found: C, 64.22; H, 6.50; N, 6.65%.

**Synthesis of Fe3.** Using the same procedure as described for the synthesis of **Fe1** with **L3** as the ligand, **Fe3** was obtained as a green powder (0.13 g, 56%). FT-IR (KBr,  $cm^{-1}$ ): 3309 (w,  $\nu_{OH}$ ), 2969 (w), 2932 (w), 2874 (w), 1688 (w), 1617 (m,  $\nu_{C=N}$ ), 1587 (s), 1511 (m), 1470 (m), 1448 (s), 1371 (s), 1335 (w), 1263 (s), 1214 (s), 1172 (w), 1106 (w), 1028 (w), 976 (w), 840 (s), 808 (s), 771 (m), 739 (w), 675 (w), 611 (w), 525 (w), 434 (w). Anal. Calcd. for  $C_{61}H_{66}Cl_4Fe_2N_6O$  (1150.28): C, 63.56; H, 5.77; N, 7.29. Found: C, 63.26; H, 5.99; N, 6.92%.

**Synthesis of Fe4.** Using the same procedure as described for the synthesis of **Fe1** with **L4** as the ligand, **Fe4** was obtained as a green powder (0.19 g, 79%). FT-IR (KBr,  $cm^{-1}$ ): 3332 (w,  $\nu_{OH}$ ), 2962 (m), 2925 (w), 2867 (w), 1690 (w), 1616 (m,  $\nu_{C=N}$ ), 1586 (s), 1510 (m), 1464 (s), 1439 (s), 1366 (s), 1322 (w), 1263 (s), 1214 (s), 1173 (w), 1104 (w), 1027 (w), 836 (s), 803 (s), 767 (m), 673 (w), 594 (w), 524 (w), 476 (w), 438 (w), 419 (w). Anal. Calcd. for  $C_{65}H_{74}Cl_4Fe_2N_6O$  (1206.34): C, 64.58; H, 6.17; N, 6.95. Found: C, 64.97; H, 6.32; N, 6.61%.

**Synthesis of Fe5.** Using the same procedure as described for the synthesis of **Fe1** with **L5** as the ligand, **Fe5** was obtained as a green powder (0.20 g, 89%). FT-IR (KBr,  $cm^{-1}$ ): 3310 (w,  $\nu_{OH}$ ), 2960 (w), 2915 (w), 2857 (w), 1697 (w), 1614 (w,  $\nu_{C=N}$ ), 1587 (s), 1512 (m), 1475 (s), 1438 (m), 1370 (s), 1263 (s), 1263 (s), 1216 (s), 1173 (w), 1101 (w), 1028 (w), 850 (m), 810 (s), 736 (m). Anal. Calcd. for  $C_{59}H_{62}Cl_4Fe_2N_6O$  (1124.68): C, 63.01; H, 5.56; N, 7.47. Found: C, 62.77; H, 5.31; N, 7.11%.

**Synthesis of Fe6.** Using the same procedure as described for the synthesis of **Fe1** with **L6** as the

ligand, **Fe6** was obtained as a green powder (0.22 g, 87%). FT-IR (KBr,  $\text{cm}^{-1}$ ): 3240 (w,  $\nu_{\text{OH}}$ ), 2965 (m), 2928 (w), 2873 (w), 1699 (w), 1613 (m,  $\nu_{\text{C=N}}$ ), 1585 (s), 1512 (m), 1459 (s), 1371 (s), 1364 (s), 1213 (s), 1173 (w), 1151 (w), 1101 (w), 1027 (w), 854 (m), 806 (s), 735 (m). Anal. Calcd. for  $\text{C}_{67}\text{H}_{78}\text{Cl}_4\text{Fe}_2\text{N}_6\text{O}$  (1236.89): C, 65.06; H, 6.36; N, 6.79. Found: C, 65.19; H, 6.00; N, 6.57%.

### **Ethylene polymerization at 5 or 10 atm $\text{C}_2\text{H}_4$**

The polymerizations at 5 or 10 atm  $\text{C}_2\text{H}_4$  were carried out in a 250 mL stainless steel autoclave equipped with a mechanical stirrer and temperature controller. In addition, the reactor was equipped with a thermocouple to detect the reaction temperature and some control of any exotherm generated could be achieved by adjusting the water flow in the steel tube inside the autoclave. The autoclave was evacuated and refilled with nitrogen two times and then with ethylene one time. The precatalyst were then dispersed in toluene by using ultrasonic shaking due to its poor solubility in toluene. When the required temperature was reached, the precatalyst (2.0  $\mu\text{mol}$  for MAO and 1.5  $\mu\text{mol}$  for MMAO) in toluene (25 mL) was injected into the autoclave under an ethylene atmosphere (*ca.* 1 atm). Any residual precatalyst was washed into the autoclave with toluene followed by the addition of more toluene (50 mL). The required amount of co-catalyst (MAO, MMAO) and additional toluene were added successively by syringe taking the total volume of solvent to 100 mL. The autoclave was immediately pressurized with 5/10 atm  $\text{C}_2\text{H}_4$  and the stirring commenced. After the required reaction time, the reactor was cooled with an ice/water bath and the excess ethylene released. The reaction was then quenched with 10% hydrochloric acid in ethanol and the precipitated polymer collected, washed with ethanol and then dried under reduced pressure at 50  $^{\circ}\text{C}$  to constant weight and weighed.

### Ethylene polymerization at 1 atm ethylene pressure.

The polymerization at 1 atm C<sub>2</sub>H<sub>4</sub> was carried out in a Schlenk tube. Under an ethylene atmosphere (1 atm), **Fe1** (2.0 μmol for MAO and 1.5 μmol for MMAO) was added followed by toluene (30 mL) and then the required amount of co-catalyst (MAO, MMAO) introduced by syringe. The resulting solution was stirred at 60 °C under 1 atm C<sub>2</sub>H<sub>4</sub>. After 30 min, the pressure was vented and the mixture quenched with 10% hydrochloric acid in ethanol. The polymer was washed with ethanol, dried under reduced pressure at 50 °C and then weighed.

### Crystallographic studies

An X-ray diffraction study on a crystal of **Fe6** was carried out on using a Rigaku Sealed Tube CCD (Saturn 724+) diffractometer with graphite-monochromated Mo-K<sub>α</sub> radiation ( $\lambda = 0.71073 \text{ \AA}$ ) at 173(2) K; the cell parameters were obtained by global refinement of the positions of all collected reflections. Intensities were corrected for Lorentz and polarization effects and empirical absorption. The structure was solved by direct methods and refined by full-matrix least-squares on  $F^2$ . All non-hydrogen atoms were refined anisotropically and all hydrogen atoms were placed in calculated positions. Structure solution was performed using SHELXT (Sheldrick, 2015)<sup>26a</sup> and structure refinement performed using SHELXL (Sheldrick, 2015).<sup>26b</sup> During the structural refinement, the solvent was squeezed (**Fe6**) with PLATON software.<sup>27</sup> Crystal data and processing parameters for **Fe6** are summarized in Table 4.

**Table 4** Crystal data and structure refinement details for **Fe6**

Empirical formula	C <sub>67</sub> H <sub>78</sub> Cl <sub>4</sub> Fe <sub>2</sub> N <sub>6</sub> O
Formula weight	1236.85
Temperature/K	173.15
Wavelength/Å	0.71073

Crystal system	monoclinic
Space group	P2 <sub>1</sub> /c
a/Å	23.6388(8)
b/Å	17.3226(3)
c/Å	18.5225(5)
Alpha/°	90
Beta/°	93.052(3)
Gamma/°	90
Volume/Å <sup>3</sup>	7573.9(4)
Z	4
Dcalcd/(g cm <sup>-3</sup> )	1.085
μ/mm <sup>-1</sup>	0.563
F(000)	2600.0
Crystal size/mm <sup>3</sup>	0.126 × 0.068 × 0.056
θ range/°	3.222–53
	-29 ≤ h ≤ 29
Limiting indices	-21 ≤ k ≤ 21
	-23 ≤ l ≤ 23
No. of rflns collected	125676
No. unique rflns	23928
R(int)	0.1217
No. of params	778
Completeness to θ	1.000
Goodness of fit on F <sup>2</sup>	1.126
Final R indices [I ≥ 2σ(I)]	R <sub>1</sub> = 0.1041
	wR <sub>2</sub> = 0.2224
R indices (all data)	R <sub>1</sub> = 0.1453
	wR <sub>2</sub> = 0.2444
Largest diff. peak and hole/(e Å <sup>-3</sup> )	0.98/-0.29

## ASSOCIATED CONTENT

The Supporting Information is available free of charge on the ACS Publications website at DOI:10.1021/om\_\_\_\_. X-ray crystallographic data in CIF for CCDC 1862881 (**Fe6**) available free of charge from The Cambridge Crystallographic Data Centre

## AUTHOR INFORMATION

### Corresponding Author

\*E-mail: whsun@iccas.ac.cn; Tel: +86-10-62557955; Fax: +86-10-62618239 (W.-H.S).

\*E-mail: zhangwj@bift.edu.cn; Tel: +86-10-62659707 (W.Z.)

\*E-mail: gas8@leicester.ac.uk; Tel: +44-116-2522096 (G.A.S.)

## Notes

The authors declare no competing financial interest.

## ACKNOWLEDGMENTS

This work was supported by the National Natural Science Foundation of China (Nos. 51473170, and 21871275). GAS thanks the Chinese Academy of Sciences for a President's International Fellowship for Visiting Scientists.

## REFERENCES

- (1) (a) Small, B. L.; Brookhart, M.; Bennett, A. M. A. Highly Active Iron and Cobalt Catalysts for the Polymerization of Ethylene. *J. Am. Chem. Soc.* **1998**, *120*, 4049-4050; (b) Britovsek, G. J. P.; Gibson, V. C.; Kimberley, B. S.; Maddox, P. J.; McTavish, S. J.; Solan, G. A.; White, A. J. P. and Williams, D. J. Iron-Based Catalysts with Exceptionally High Activities and Selectivities for Oligomerization of Ethylene to Linear  $\alpha$ -Olefins. *Chem. Commun.*, **1998**, 849–850.
- (2) (a) Gibson, V. C.; Redshaw, C.; Solan, G. A. Bis(imino)pyridines: Surprisingly Reactive Ligands and a Gateway to New Families of Catalysts. *Chem. Rev.* **2007**, *107*, 1745-1776; (b) Gibson, V. C.; Solan, G. A. Iron-Based and Cobalt-Based Olefin Polymerisation Catalysts. *Top.*

*Organomet. Chem.* **2009**, *26*, 107–158; (c) Gibson, V. C.; Solan, G. A. Olefin Oligomerizations and Polymerizations Catalyzed by Iron and Cobalt Complexes Bearing Bis(imino)pyridine Ligands. in *Catalysis without Precious Metals* (Ed. M. Bullock), Wiley-VCH, Weinheim, **2010**, 111–141; (d) Xiao, T.; Zhang, W.; Lai, J.; Sun, W.-H. Iron-oriented ethylene oligomerization and polymerization: The Iron Age or a flash in the pan. *C.R. Chim.*, **2011**, *14*, 851-855; (e) Ma, J.; Feng, C.; Wang, S.; Zhao, K.; Sun, W.-H.; Redshaw, C.; Solan, G. A. Bi- and tri-dentate imino-based iron and cobalt pre-catalysts for ethylene oligo-/polymerization. *Inorg. Chem. Front.*, **2014**, *1*, 14-34; (f) Flisak, Z.; Sun, W.-H. Progression of Diiminopyridines: From Single Application to Catalytic Versatility. *Acs Catalysis*, **2015**, *5*, 4713-4724; (g) Ma, Z.; Yang, W.; Sun, W.-H. Recent Progress on Transition Metal (Fe, Co, Ni, Ti and V) Complex Catalysts in Olefin Polymerization with High Thermal Stability. *Chin. J. Chem.*, **2017**, *35*, 531-540; (h) Wang, Z.; Solan, G. A.; Zhang, W.; Sun, W.-H. Carbocyclic-fused *N,N,N*-pincer ligands as ring-strain adjustable supports for iron and cobalt catalysts in ethylene oligo-/polymerization. *Coord. Chem. Rev.*, **2018**, *363*, 92-108.

(3) (a) Delferro, M.; Marks, T. J. Multinuclear Olefin Polymerization Catalysts. *Chem. Rev.*, **2011**, *111*, 2450-2485; (b) Suo, H.; Solan, G. A.; Ma, Y.; Sun, W.-H. Developments in compartmentalized bimetallic transition metal ethylene polymerization catalysts. *Coord. Chem. Rev.*, **2018**, *372*, 101-116.

(4) (a) Bianchini, C.; Giambastiani, G.; Rios, I. G.; Meli, A.; Oberhauser, W.; Sorace, L.; Toti, A. Synthesis of a New Polydentate Ligand Obtained by Coupling 2,6-Bis(imino)pyridine and (Imino)pyridine Moieties and Its Use in Ethylene Oligomerization in Conjunction with Iron(II)

- and Cobalt(II) Bis-halides. *Organometallics*, **2007**, *26*, 5066-5078; (b) Zhang, S.; Sun, W.-H.; Kuang, X.; Vystorop, I.; Yi, J. Unsymmetric bimetal(II) complexes: Synthesis, structures and catalytic behaviors toward ethylene. *J. Organomet. Chem.*, **2007**, *692*, 5307-5316; (c) Zhang, S.; Vystorop, I.; Tang, Z.; Sun, W.-H. Bimetallic (Iron or Cobalt) Complexes Bearing 2-Methyl-2,4-bis(6-iminopyridin-2-yl)-1H-1,5-benzodiazepines for Ethylene Reactivity. *Organometallics*, **2007**, *26*, 2456-2460; (d) Armitage, A. P.; Champouret, Y. D. M.; Grigoli, H.; Pelletier, J. D. A.; Singh, K.; Solan, G. A. Probing the Effect of Binding Site and Metal Centre Variation in Pentadentate Oligopyridylimine-Bearing Bimetallic (Fe<sub>2</sub>, Co<sub>2</sub>, Ni<sub>2</sub>) Ethylene Oligomerisation Catalysts. *Eur. J. Inorg. Chem.*, **2008**, 4597-4607; (e) Sun, W.-H.; Xing, Q.; Yu, J.; Novikova, E.; Zhao, W.; Tang, X.; Liang, T.; Redshaw, C. Probing the Characteristics of Mono- or Bimetallic (Iron or Cobalt) Complexes Bearing 2,4-Bis(6-iminopyridin-2-yl)-3H-benzazepines: Synthesis, Characterization, and Ethylene Reactivity. *Organometallics*, **2013**, *32*, 2309-2318.
- (5) Barbaro, P.; Bianchini, C.; Giambastiani, G.; Rios, I. G.; Meli, A.; Oberhauser, W.; Segarra, A. M.; Sorace, L.; Toti, A. Synthesis of New Polydentate Nitrogen Ligands and Their Use in Ethylene Polymerization in Conjunction with Iron(II) and Cobalt(II) Bis-halides and Methylaluminoxane. *Organometallics*, **2007**, *26*, 4639-4651.
- (6) Liu, J.; Li, Y.; Liu, J.; Li, Z. Ethylene Polymerization with a Highly Active and Long-Lifetime Macrocyclic Trinuclear 2,6-Bis(imino)pyridyliron. *Macromolecules*, **2005**, *38*, 2559-2563.
- (7) Wang, L.; Sun, J. Methylene bridged binuclear bis(imino)pyridyl iron(II) complexes and their use as catalysts together with Al(*i*-Bu)<sub>3</sub> for ethylene polymerization. *Inorg. Chim. Acta*, **2008**,

361, 1843-1849.

- (8) Xing, Q.; Zhao, T.; Qiao, Y.; Wang, L.; Redshaw, C.; Sun, W.-H. Synthesis, characterization and ethylene polymerization behavior of binuclear iron complexes bearing N,N'-bis(1-(6-(1-(arylimino)ethyl) pyridin-2-yl)-ethylidene)benzidines. *RSC Adv.*, **2013**, *3*, 26184-26193.
- (9) Takeuchi, D.; Takano, S.; Takeuchi, Y.; Osakada, K. Ethylene Polymerization at High Temperatures Catalyzed by DoubleDecker-Type Dinuclear Iron and Cobalt Complexes: Dimer Effect on Stability of the Catalyst and Polydispersity of the Product. *Organometallics*, **2014**, *33*, 5316-5323.
- (10) (a) Guo, D.; Han, L.; Zhang, T.; Sun, W.-H.; Li, T.; Yang, X. Temperature Dependence of the Activity of a Late Transition Metal Catalyst by Molecular Modeling. *Macromol. Theory Simul.*, **2002**, *11*, 1006-1012; (b) Zhang, T.; Guo, D.; Jie, S.; Sun, W.-H.; Li, T.; Yang, X. Influence of Electronic Effect on Catalytic Activity of Salicylaldiminato Nickel(II) Complexes. *J. Polym. Sci., Part A: Polym. Chem.*, **2004**, *42*, 4765-4774; (c) Yang, W.; Yi, J.; Sun, W.-H. Revisiting Benzylidenequinolinylnickel Catalysts through the Electronic Effects on Catalytic Activity by DFT Studies. *Macromol. Chem. Phys.*, **2015**, *216*, 1125-1133.
- (11) (a) Maruoka, K.; Imoto, H.; Saito, S.; Yamamoto, H. Virtually Complete Blocking of  $\alpha$ ,  $\beta$ -Unsaturated Aldehyde Carbonyls by Complexation with Aluminum Tris(2,6-diphenylphenoxide). *J. Am. Chem. Soc.*, **1994**, *116*, 4131-4132; (b) Cloete, J.; Mapolie, S. F. Functionalized pyridinyl-imine complexes of palladium as catalyst precursors for ethylene polymerization. *J. Mol. Catal. A: Chem.*, **2006**, *243*, 221-225.

- (12) (a) Schrekker, H. S.; Kotov, V.; Preishuber-Pflugl, P.; White, P.; Brookhart, M. Efficient Slurry-Phase Homopolymerization of Ethylene to Branched Polyethylenes Using R-Diimine Nickel(II) Catalysts Covalently Linked to Silica Supports. *Macromolecules*, **2006**, *39*, 6341-6354; (b) Hu, T.; Li, Y.-G.; Liu, J.-Y.; Li, Y.-S. Syntheses and Ethylene Polymerization Behavior of Supported Salicylaldimine-Based Neutral Nickel(II) Catalysts. *Organometallics*, **2007**, *26*, 2609-2615; (c) Zhang, L.; Castillejos, E.; Serp, P.; Sun, W.-H.; Durand, J. Enhanced ethylene polymerization of Ni(II) complexes supported on carbon nanotubes. *Catal. Today*, **2014**, *235*, 33-40.
- (13) Chen, Q.; Zhang, W.; Solan, G. A.; Liang, T.; Sun, W.-H. Methylene-bridged bimetallic bis(imino)pyridinecobaltous chlorides as precatalysts for vinylterminated polyethylene waxes. *Dalton Trans.*, **2018**, *47*, 6124-6133.
- (14) (a) Yu, J.; Liu, H.; Zhang, W.; Hao, X.; Sun, W.-H. Access to highly active and thermally stable iron procatalysts using bulky 2-[1-(2,6-dibenzhydryl-4-methylphenylimino)ethyl]-6-[1-(arylimino)ethyl]pyridine ligands. *Chem. Commun.*, **2011**, *47*, 3257-3259; (b) Du, S.; Wang, X.; Zhang, W.; Flisak, Z.; Sun, Y.; Sun, W.-H. A practical ethylene polymerization for vinyl-polyethylenes: synthesis, characterization and catalytic behavior of  $\alpha,\alpha'$ -bisimino-2,3:5,6-bis(pentamethylene)pyridyliron chlorides. *Polym. Chem.*, **2016**, *7*, 4188-4197; (c) Zhang, Y.; Suo, H.; Huang, F.; Liang, T.; Hu, X.; Sun, W.-H. Thermo-Stable 2-(Arylimino)benzylidene-9-arylimino-5,6,7,8-tetrahydro cyclohepta[b]pyridyliron(II) Precatalysts Toward Ethylene Polymerization and Highly Linear Polyethylenes. *J. Polym. Sci., Part A: Polym. Chem.*, **2017**, *55*, 830-842.

- (15) Kim, I.; Han, B. H.; Ha, C.-S.; Kim, J.-K.; Suh, H. Preparation of Silica-Supported Bis(imino)pyridyl Iron(II) and Cobalt(II) Catalysts for Ethylene Polymerization. *Macromolecules*, **2003**, *36*, 6689-6691.
- (16) Britovsek, G. J. P.; Bruce, M.; Gibson, V. C.; Kimberley, B. S.; Maddox, P. J.; Mastroianni, S.; McTavish, S. J.; Redshaw, C.; Solan, G. A.; Strömberg, S.; White, A. J. P.; Williams, D. J. Iron and Cobalt Ethylene Polymerization Catalysts Bearing 2,6-Bis(Imino)Pyridyl Ligands: Synthesis, Structures, and Polymerization Studies *J. Am. Chem. Soc.*, **1999**, *121*, 8728-8740.
- (17) Xiao, T.; Hao, P.; Kehr, G.; Hao, X.; Erker, G.; Sun, W.-H. Dichlorocobalt(II) Complexes Ligated by Bidentate 8-(Benzoimidazol-2-yl)quinolines: Synthesis, Characterization, and Catalytic Behavior toward Ethylene. *Organometallics*, **2011**, *30*, 4847-4853.
- (18) Galland, G. B.; Quijada, R.; Rojas, R.; Bazan, G.; Komon, Z. J. A. NMR Study of Branched Polyethylenes Obtained with Combined Fe and Zr Catalysts. *Macromolecules*, **2002**, *35*, 339-345.
- (19) (a) Ma, Z.; Wang, H.; Qiu, J.; Xu, D.; Hu, Y. A Novel Highly Active Iron/2,6-Bis(imino)pyridyl Catalyst for Ethylene Polymerization. *Macromol. Rapid Commun.*, **2001**, *22*, 1280-1283; (b) Britovsek, G. J. P.; Mastroianni, S.; Solan, G. A.; Baugh, S. P. D.; Redshaw, C.; Gibson, V. C.; White, A. J. P.; Williams, D. J.; Elsegood, M. R. J. Oligomerization of Ethylene by Bis(imino)pyridyliron and -cobalt Complexes. *Chem. Eur. J.*, **2000**, *6*, 2221-2231.
- (20) Huang, F.; Zhang, W.; Yue, E.; Liang, T.; Hu, X.; Sun, W.-H. Controlling the molecular weights of polyethylene waxes using the highly active precatalysts of

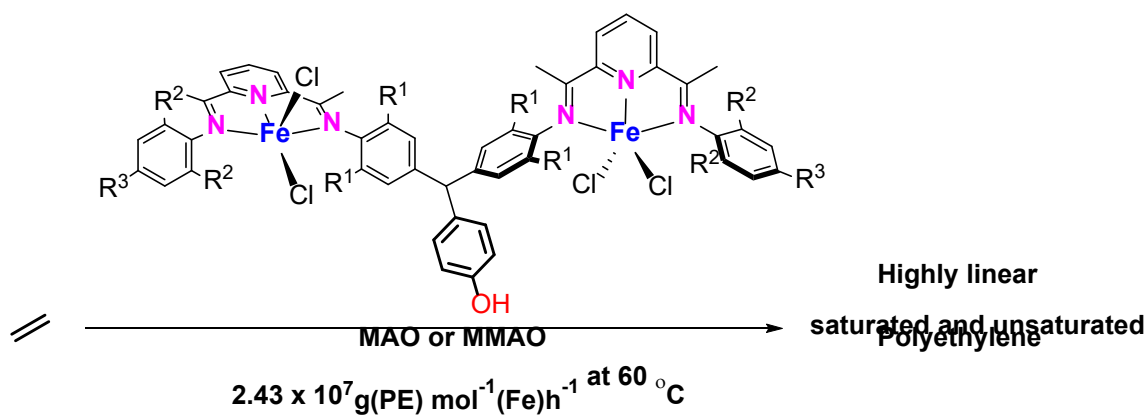
- 2-(1-aryliminoethyl)-9-arylimino-5,6,7,8-tetrahydrocycloheptapyridylcobalt chlorides: synthesis, characterization, and catalytic behavior. *Dalton Trans.*, **2016**, *45*, 657-666.
- (21) Semikolenova, N. V.; Sun, W.-H.; Soshnikov, I. E.; Matsko, M. A.; Kolesova, O. V.; Zakharov, V. A.; Bryliakov, K. P. Origin of “Multisite-like” Ethylene Polymerization Behavior of the Single-Site Nonsymmetrical Bis(imino)pyridine Iron(II) Complex in the Presence of Modified Methylaluminumoxane. *ACS Catal.*, **2017**, *7*, 2868-2877.
- (22) (a) Sun, W.-H.; Tang, X.; Gao, T.; Wu, B.; Zhang, W.; Ma, H. Synthesis, Characterization, and Ethylene Oligomerization and Polymerization of Ferrous and Cobaltous 2-(Ethylcarboxylato)-6-iminopyridyl Complexes. *Organometallics*, **2004**, *23*, 5037-5047; (b) Huang, F.; Zhang, W.; Sun, Y.; Hu, X.; Solan, G. A.; Sun, W.-H. Thermally stable and highly active cobalt precatalysts for vinyl-polyethylenes with narrow polydispersities: integrating fused-ring and imino-carbon protection into ligand design. *New J. Chem.*, **2016**, *40*, 8012-8023.
- (23) Kissin, Y. V.; Qian, C., Xie, G.; Chen, Y. Multi-Center Nature of Ethylene Polymerization Catalysts Based on 2,6-Bis(imino)pyridyl Complexes of Iron and Cobalt. *J. Polym. Sci., Part A: Polym. Chem.*, **2006**, *44*, 6159-6170.
- (24) (a) Cao, X.; He, F.; Zhao, W.; Cai, Z.; X. Hao; Shiono, T.; Redshaw, C.; Sun, W.-H. 2-[1-(2,6-Dibenzhydryl-4-chlorophenylimino)ethyl]-6-[1-(arylimino)ethyl]pyridyliron(II) dichlorides: Synthesis, characterization and ethylene polymerization behavior. *Polymer*, **2012**, *53*, 1870-1880; (b) Sun, W.-H.; Zhao, W.; Yu, J.; Zhang, W.; Hao, X.; Redshaw, C. Enhancing the Activity and Thermal Stability of Iron Precatalysts Using 2-(1-{2,6-bis[bis(4-fluorophenyl)methyl]-4-methylphenylimino}ethyl)-6-[1-(arylimino)ethyl]py

- ridines. *Macromol. Chem. Phys.*, **2012**, *213*, 1266-1273; (c) Zhao, W.; Yu, J.; Song, S.; Yang, W.; Liu, H.; Hao, X.; Redshaw, C.; Sun, W.-H. Controlling the ethylene polymerization parameters in iron pre-catalysts of the type 2-[1-(2,4-dibenzhydryl-6-methylphenylimino)ethyl]-6-[1-(arylimino)ethyl]pyridyliron dichloride. *Polymer*, **2012**, *53*, 130-137; (d) Zhang, W.; Wang, S.; Du, S.; Guo, C.-Y.; Hao, X.; Sun, W.-H. 2-(1-(2,4-Bis((di(4-fluorophenyl)methyl)-6-methylphenylimino)ethyl)-6-(1-(arylimino)ethyl)pyridylmetal (iron or cobalt) Complexes: Synthesis, Characterization, and Ethylene Polymerization Behavior. *Macromol. Chem. Phys.*, **2014**, *215*, 1797-1809.
- (25) (a) Solan, G. A.; Pelletier, J. D. Transition Metal Compounds for Olefin Polymerization and Oligomerization. A. WO2005/118605(A1), **2005**; (b) Bianchini, C.; Mantovani, G.; Meli, A.; Migliacci, F.; Zanobini, F.; Laschi, F.; Sommazzi, A. Oligomerisation of ethylene to linear alpha-olefins by new C<sub>s</sub>- and C<sub>1</sub>-symmetric [2,6-bis(imino)pyridyl] iron and -cobalt dichloride complexes. *Eur. J. Inorg. Chem.*, **2003**, *8*, 1620-1631.
- (26) (a) Sheldrick, G. M. SHELXT-Integrated space-group and crystal-structure determination. *Acta Cryst.* **2015**, *A71*, 3-8; (b) Sheldrick, G. M.; SHELXT-Integrated space-group and crystal-structure determination. *Acta Cryst.* **2015**, *C71*, 3
- (27) Spek, L. Structure validation in chemical crystallography. *Acta Crystallogr., Sect. D: Biol. Crystallogr.*, **2009**, *65*, 148.

For the Table of Contents use only

## CH(phenol)-bridged bis(imino)pyridines as compartmental supports for diiron precatalysts for ethylene polymerization: exploring cooperative effects on performance

Qiang Chen,<sup>†</sup> Wenjuan Zhang,<sup>†,‡,\*</sup> Gregory A. Solan,<sup>†,§,\*</sup> Randi Zhang,<sup>†</sup> Liwei Guo,<sup>‡</sup> Xiang Hao,<sup>†</sup> and Wen-Hua Sun<sup>†,\*</sup>



Bimetallic catalysts for ethylene polymerization are disclosed which display good thermal stability, very high activity and moreover highlight the importance of the diiron core and the phenol unit on performance.